Physicochemical studies on reaction mechanism of molecular chaperone GroE

分子シャペロン GroE の反応機構に関する物理化学的研究

2014

So Ishino

Contents

Abbreviations 3
Preface 4

Chapter 1
Effects of C-terminal truncation of chaperonin GroEL on the yield of the in-cage folding of green fluorescent protein
Introduction 6
Materials and Methods 7
Results 11
Discussion 22

Chapter 2
The ring-exchange reaction of chaperonin GroEL probed by fluorescence resonance energy transfer
Abstract 26

Chapter 3
Evaluating the stability of an SR398/GroES chaperonin complex
Introduction 27
Materials and Methods 27
Results and Discussion 29

Conclusion 39
Acknowledgements 40
References 41

Abbreviations

ADP	adenosine 5'-triphosphate
AMPPNP	adenosine 5'-(β,γ-imido)triphosphate
ATP	adenosine 5'-triphosphate
ATPγS	adenosine 5'-[γ-thio]triphosphate
BeFx	berrium fluoride
DTT	dithiothreitol
EDTA	ethylenediaminetetraacetic acid
EL	GroEL
ELΔC	C-terminal truncated variant of GroEL
EL398	ATPase-deficient variant of GroEL (D398A)
EL52/398	ATPase-deficient variant of GroEL (D52A, D398A)
EL52/398ΔC	ATPase-deficient C-terminal truncated variant of GroEL (D52A, D398A)
ES	GroES
FRET	fluorescence resonance energy transfer
GFP	green fluorescent protein
IPTG	isopropyl β-D-thiogalactopyranoside
Ni-NTA	nickel-nitrilotriacetic acid
ORF	open reading flame
PCR	polymerase chain reaction
PEP	phospho(enol)pyruvic acid
PMSF	phenylmethylsulfonyl fluoride
Rubisco	ribulose 1,5-bisphosphate carboxylase/oxygenase
SEC	size exclusion chromatography
SR1	single-ring variant of GroEL
SR398	single-ring variant with ATPase-deficient mutation (D398A) of GroEL
SR1ΔC	C-terminal truncated single-ring variant of GroEL
TEM	transmission electron microscopy

Preface

Escherichia coli molecular chaperone GroEL and its co-chaperone GroES assist the folding of a wide variety of proteins that are essential for cell growth [1-5]. GroEL is composed of two heptameric rings of identical 57-kDa subunits, and these rings are stacked back to back [6]. The subunit of GroEL comprises three domains: the apical domain, which binds non-native substrate proteins and GroES, the equatorial domain that contains ATP-binding site, and the intermediate domain that connects the other two domains. GroES is a dome-shaped heptameric ring consisting of identical 10-kDa subunits [7]. Each GroEL ring has a large central cavity with a hydrophobic entrance for the binding of GroES and non-native substrate proteins in a competitive manner. GroEL binds GroES in the presence of ATP, resulting the encapsulation of the non-native substrate protein into the central cavity of GroEL capped by GroES (Fig. P-1 and P-2) [8, 9]. The volume of the cavity in this GroES-sealed GroEL ring (*cis*-ring) becomes doubly expanded, acting as a folding chamber in which folding of the substrate protein proceeds without intermolecular aggregation. It is widely accepted that GroE controls its reaction cycle by using the hydrolysis of ATP. The functional intermediate during the cycle has been considered as so-called the bullet-shaped complex, in which the one side of the ring of GroEL is occupied with GroES (Fig. P-2) [10]. Recently, however, the involvement of the symmetric football-shaped complex, in which both two rings of GroEL are occupied with GroES, during the reaction cycle has been presented in the presence of denatured proteins [11-13]. In addition, it was suggested that the double-ring GroEL transiently split into single rings in the presence of ATP [14, 15]. Thus, the detailed reaction cycle of GroE, including the formation of the football-shaped complex and the ring-splitting reaction, remains to be elusive. Furthermore, although the structure and function of GroE were intensively investigated by X-ray crystallographic studies, the roles of C-terminal regions of GroEL, which were not visible in the crystal structure, were not yet fully understood.

Recent studies have suggested that the C-terminal tails of GroEL plays an important role in substrate protein encapsulation [16]. In chapter 1, the author investigated the effects of C-terminal truncation on the yield of the in-cage folding of green fluorescent protein (GFP).

In chapter 2, the author investigated the ring-splitting reaction of double-ring GroEL. As a result of reassociation of transiently-split single rings, the exchange of the rings would occur, which was detected by using inter-ring fluorescence resonance energy transfer (FRET). The occurrence of the exchange reaction during the functional cycle was also analyzed.

Recently, the GroE cage has been considered as an attractive nano carrier. It has been known that the single-ring mutant with an ATPase-deficient mutation (D398A), SR398,

formed very stable complex with GroES [17]. However, the information about its stability remains to be elucidated. In chapter 3, the author investigated the stability of the SR398/GroES chaperonin cage formed in the presence of non-hydrolyzed ATP-analogue, ATPγS.

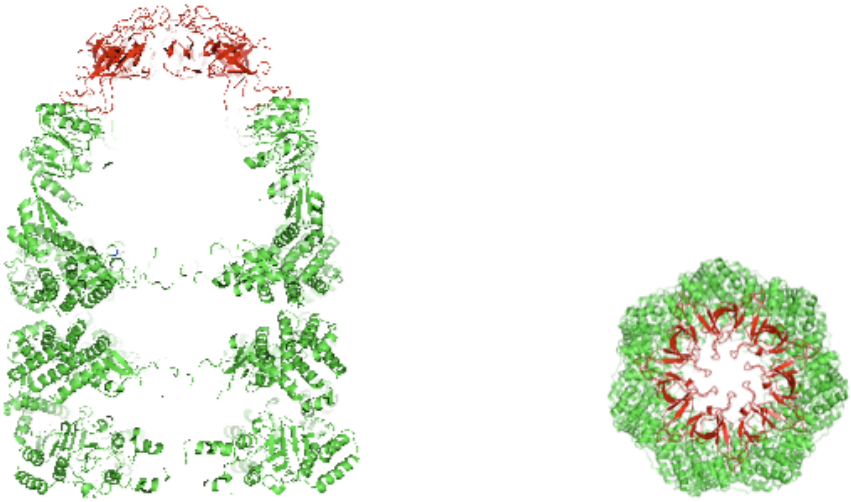

Fig. P-1. The crystal structure of the EL_{14}/ES_7 bullet-shaped complex in the presence of ADP [9]. The sliced view (left) and the top view (right) are shown. GroEL is shown in green and GroES is shown in red, respectively.

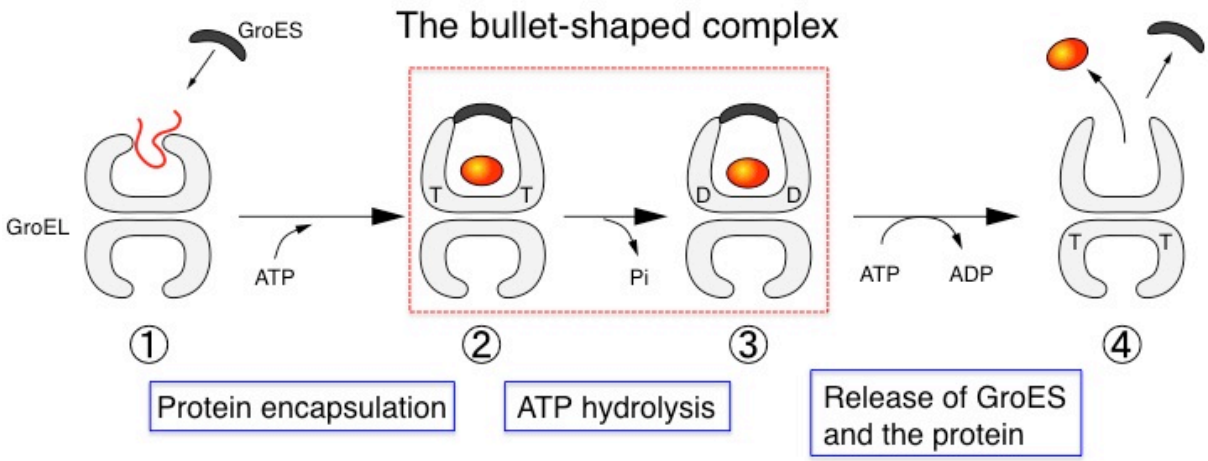

Fig. P-2. Schematic representation of the GroE-assisted protein folding mediated by the $GroEL_{14}/GroES_7$ bullet-shaped complex. The model is divided into three steps: the encapsulation of a substrate protein, the hydrolysis of ATP (abbreviated as T in the diagram) at the *cis*-ring, and the release of ADP (abbreviated as D in the diagram), GroES and the substrate protein upon binding of bulk ATP to the opposite ring.

Chapter 1

Effects of C-terminal truncation of chaperonin GroEL on the yield of the in-cage folding of green fluorescent protein

1-1. Introduction

Although the mechanism underlying GroE-assisted protein folding remains controversial whether GroE acts as a passive anti-aggregation cage [18, 19] or actively accelerates protein folding [20, 21], there is a point of agreement that both two mechanisms require efficient substrate protein encapsulation. The C-terminal tails of GroEL have recently been considered to play a key role in efficient protein encapsulation [16]. The 23 amino acid residues in the C-terminal, which are invisible in the X-ray crystal structure due to their high flexibility, have been suggested to separate the double rings at the bottom of the cavity [22-24]. Chen et al. [16] observed using cryo-electron microscopy that the C-terminal tails of GroEL interacted with the substrate protein, Rubisco, which was encapsulated within the GroE cavity. They also showed that C-terminal truncation reduced the yield of in-cage substrate folding, proving the importance of C-terminal tails for efficient protein encapsulation.

It has yet to be determined whether C-terminal tails are required for the incorporation of a substrate protein into the cavity and/or the retention of the substrate within the cage by blocking the escape of a substrate through the bottom space of the cage. Since the crystal structure of GroEL indicates that there is a large pore at the bottom of the cage, which may be covered with C-terminal tails, it is reasonable to assume that the encapsulated substrate within the cavity can escape through the pore in the absence of C-terminal tails. To clarify this point, the author investigated the effects of C-terminal truncation on GroE-mediated in-cage folding using green fluorescent protein (GFP) as a substrate.

1-2. Materials and Methods

Materials

ATP was purchased from Wako Pure Chemical Industries Ltd (Saitama, Japan). Other reagents were purchased from Nacalai Tesque (Kyoto, Japan).

Protein expression and purification

The expression plasmid of wild-type GroEL and GroES (pUCESL) was constructed as described previously [27]. To facilitate mutagenesis, the gene of wild-type GroEL and GroES was first subcloned into a pAED4 vector with 5'-*Nde* I and 3'-*Eco* RI sites to produce the pAED-EL and pAED-ES expression vector [28]. The expression vector for the single-ring

mutant of GroEL (pEL-SR1, containing the mutations R452G/E461A/S463A/V464A) was obtained as a gift from Dr. K. Kuwajima [29, 30]. The expression vectors with the double ATPase-deficient mutations of GroEL (D52A/D398A) were constructed by the QuickChange site-directed mutagenesis kit (Stratagene) using pAED-EL and pEL-SR1 as a template to produce pAED-EL52/398 and pEL-SR52/398, respectively.

The C-terminal truncated mutant for the single-ring variant of GroEL with ATPase-deficient mutations (pEL-SR52/398ΔC) was produced using PCR with appropriate 5'- and 3'-primers in which a stop codon was introduced at position K526. The other C-terminal-truncated GroEL mutants were produced by the substitution of K526 with the stop codon (AAA to TAA) using the QuickChange method with pAED-EL and pEL-SR1 as a template. The substrate-trap mutant of GroEL (N265A) was also constructed using the QuickChange method.

The vectors obtained were introduced into *E. coli* strain BL21(DE3)/pLysS (Novagen). The transformed bacteria was grown at 37 °C in Lucia broth medium containing 50 μg/mL of ampicillin. Isopropyl β-$_D$-thiogalactopyranoside (IPTG) was added to the medium when the absorbance at 600 nm reached at 0.6. After 3 h, cells were harvested by centrifugation at 5,000 g for 5 min at 4 °C. The cells were suspended in buffer A (50 mM Tris-HCl (pH 7.8), 5 mM β-mercaptoethanol, 1 mM EDTA) containing 1 mM phenylmethylsulfonyl fluoride and disrupted by sonication with intermittent pulses for 1 min (pulse of 0.5 s, interval of 0.5 s, output level of 7) by three times using an ultrasonic disruptor equipped with a TP-012 standard tip (UD-201; Tomy, Tokyo). The final concentration of 5% of streptomycin was then added to precipitate the nucleic acid. After centrifugation at 10,000g for 30 min at 4 °C, the final concentration of ammonium sulfate was added to the supernatant to precipitate the proteins. The precipitated proteins were collected by centrifugation at 10,000 g for 2 h at 4 °C. The pellet was dissolved in 5 mL of buffer A, and applied to gel-filtration chromatography using Sephacryl-S300 column, equilibrated with buffer A containing 10% (w/v) glycerol. The fraction containing GroEL was collected, and applied to anion-exchange chromatography using Q-sepharose column, equilibrated with buffer A containing 10% (w/v) glycerol. The proteins were eluted by a linear gradient of NaCl. After purification with anion-exchange chromatography, the proteins were concentrated and loaded onto a Superdex-200 column (GE Healthcare), equilibrated with buffer B (50 mM Tris-HCl (pH 7.8), 1 mM EDTA) containing 30% (v/v) methanol [31]. The protein was dialyzed against buffer A containing 20% (w/v) glycerol, frozen by liquid nitrogen, and stored at −80°C.

The expression and purification of GroES was performed in almost the same way as that of GroEL with an additional purification step as follows. After the gel filtration chromatography step by using Sephacryl-S300 column, proteins were heated at 80°C for 20

min, and subsequently cooled at 0 °C for 30 min to refold GroES [32]. Impurities that could not refold and aggregated irreversibly were removed by centrifugation (10,000 g, 40 min, 4°C) and the supernatant was loaded onto a Q-sepharose anion-exchange column (GE Healthcare). The eluted protein was dialyzed against buffer A containing 20% (w/v) glycerol, frozen by liquid nitrogen, and stored at −80 °C.

The expression plasmid for the substrate protein, GFP with an F64L/S65T mutation, was provided by the National BioResource Project (NIG, Japan): E. coli [33]. The obtained vector, pGreenTIR, was first mutated silently to remove the *Nde* I site (CATATG to CACATG) in the ORF region by the QuickChange method (Novagen). The GFP gene was then subcloned into a pET28a (Invitrogen) vector with 5'-*Nde* I and 3'-*Eco* RI sites. The obtained expression vector encoding GFP with an N-terminal hexahistidine-tag (pET-GFP) was introduced into *E. coli* strain BL21(DE3)/pLysS. Transformed bacteria were grown in Lucia broth medium containing 25 μg/mL of kanamycin. Bacterial cells were grown at 37 °C, isopropyl-β-D-thiogalactopyranoside (IPTG) was added to the medium when the absorbance at 600 nm reached 0.6, and cells were further incubated for 3 h. Cells were harvested by centrifugation at 5,000 g for 15 min at 4 °C. The bacterial cells collected were suspended in buffer B (300 mM NaCl, 50 mM sodium phosphate, pH 8.0) containing 1 mM phenylmethanesulfonyl fluoride, and disrupted by sonication with intermittent pulses for 1 min (pulse of 0.5 s, interval of 0.5 s, output level of 7) three times using an ultrasonic disruptor UD-201 (Tomy, Tokyo, Japan) equipped with a TP-012 standard tip. Cell debris was removed by centrifugation at 10,000 g for 60 min at 4 °C, and the cell extract was loaded onto HisTrap FF (GE Healthcare). The column was washed with buffer B containing 20 mM imidazole, and bound protein was eluted with buffer B containing 150 mM imidazole and stored at 4 °C.

Transmission electron microscopy observation

Samples were applied onto carbon-coated grids, and negatively stained with 2% (w/v) uranyl acetate. Specimens were examined in a JEOL JEM 3200FSC electron microscope equipped with an Ω-type energy filter, and a field-emission electron gun operated at 200 kV. Zero energy-loss images, with a slit setting to remove electrons of an energy-loss larger than 10 eV, were recorded on a 4,096 × 4,096 15 μm/pixel slow-scan CCD camera, TemCam-F415MP (TVIPS), at a magnification of around 143,964 ×.

GFP folding reaction

GFP folding reactions were performed as follows. GFP in buffer A (50 mM Tris-HCl (pH 7.8), 10 mM KCl, 10 mM $MgCl_2$, 1 mM DTT) was denatured by the addition of HCl at a final concentration of 25 mM. A total of 182 μL of acid-denatured GFP was then diluted into a

10-fold volume of buffer A containing excess amounts of GroEL and GroES, which had been incubated at 25°C with continuous stirring in a 1-cm-quartz cell for a fluorescence spectrophotometer. After 200 sec, the addition of ATP at a final concentration of 2 mM triggered the initiation of the GFP folding reaction mediated by GroE. The recovery of GFP fluorescence at 509 nm was continuously monitored by the RF-5300PC fluorescence spectrophotometer with an excitation wavelength at 450 nm and response at 0.02 sec (SHIMADZU, Japan). The spontaneous refolding of GFP was essentially performed as described above by diluting the acid-denatured GFP into buffer A without GroEL and GroES. When indicated, BeFx (1 mM $BeCl_2$, 10 mM NaF) was included in the reaction mixture. The final concentration of GFP was 0.1 μM. The final concentrations of GroEL was as follows, 0.4 μM for wild-type GroEL (WT-EL), 1.0 μM for C-terminal truncated double-ring GroEL (ELΔC), 0.8 μM for single-ring GroEL (SR1), 2.0 μM C-terminal truncated single-ring GroEL (SR1ΔC), 0.2 μM for ATPase-deficient double-ring GroEL (EL52/398), 1.0 μM C-terminal truncated ATPase-deficient double-ring GroEL (EL52/398ΔC), 0.4 μM for ATPase-deficient single-ring GroEL (SR52/398), and 2.0 μM for C-terminal truncated ATPase-deficient single-ring GroEL (SR52/398ΔC). In each case, a two-fold molar excess of GroES (ES) per EL ring was used. When indicated, the N265A substrate-trap mutant of GroEL (0.5 μM) was included in the GFP folding reaction mediated by SR1ΔC/ES (0.05 μM GFP, 1.0 μM SR1ΔC, 2.0 μM ES). In this case, the substrate-trap mutant was added to the reaction mixture 10 sec before the addition of ATP.

Evaluation of the encapsulation yield of GFP

After monitoring the refolding reaction of GFP with a fluorescence spectrophotometer, an aliquot (50 μL) of the sample was taken to analyse the encapsulation yield by LC-10Ai gel-filtration chromatography (Shimadzu, Kyoto, Japan) equipped with a Superdex-200 HR 10/30 column (GE Healthcare). The sample was taken 25 min after the initiation of folding of GFP (the addition of ATP). In the case that the substrate-trap mutant (EL-N265A) was included in the reaction mixture, the sample was taken 300 sec after the addition of ATP.

The column was equilibrated with buffer A, which did not contain 1 mM DTT, and the protein was eluted at a flow-rate of 0.4 mL/min. When indicated, BeFx (1 mM $BeCl_2$, 10 mM NaF) was included in the running buffer. The reaction mixture was also analyzed after being incubated for 145 min. The elution of GroEL and GroES was monitored by absorption at 220 nm with the SPD-20AV absorbance detector (Shimadzu, Kyoto, Japan), while that of EL/ES/GFP ternary complex and free GFP was monitored by fluorescence at 509 nm with excitation at 450 nm using the RF-20AXS fluorescence detector (Shimadzu, Kyoto, Japan).

The encapsulation yields of GFP (E_{GFP}) were calculated by equation [1],

$$E_{\mathrm{GFP}}(\%) = \frac{N_{\mathrm{in}}}{N_{\mathrm{in}} + N_{\mathrm{out}}} \times 100 = \frac{A_{25\mathrm{min}}}{A_{25\mathrm{min}} + A_{40\mathrm{min}}} \times \frac{I_{\infty}}{I_{\infty} - I_0} \times 100 \quad [1].$$

where N_{in} and N_{out} are the number of molecules that refold within and outside of the EL/ES cage, $A_{25\mathrm{min}}$ and $A_{40\mathrm{min}}$ are the peak areas of GFP fluorescence eluted at 25 min and 40 min during size-exclusion chromatography, I_0 and I_{∞} represent the fluorescence intensities of GFP just before the addition of ATP and after completing the folding reactions, respectively. The relationships between N_{in}, N_{out}, and N_{spon} (the number of molecules that refold spontaneously regardless of EL/ES) and $A_{25\mathrm{min}}$, $A_{40\mathrm{min}}$, I_0, and I_{∞} were as follows.

$$\begin{aligned} A_{25\mathrm{min}} &\propto N_{\mathrm{in}} \\ A_{40\mathrm{min}} &\propto N_{\mathrm{out}} + N_{\mathrm{spon}} \\ I_0 &\propto N_{\mathrm{spon}} \\ I_{\infty} &\propto N_{\mathrm{in}} + N_{\mathrm{out}} + N_{\mathrm{spon}} \end{aligned}$$

These relationships proved the second equality in equation [1].

Comparison of encapsulation yields of GFP by bullet- and football-shaped GroE complexes

WT-EL or ELΔC was first mixed with two-fold molar excess amounts of GroES to form an asymmetric bullet-shaped complex in the presence of 2 mM ADP. To remove contaminated ATP, hexokinase and glucose were added at 40 U/ml and 50 mM (final concentrations), respectively, to the 20 mM of stock solution of ADP, and incubated for 5 min before use [34]. The bullet-shaped complex was then isolated by gel-filtration chromatography with the Superdex-200 HR 10/30 column (GE Healthcare), which was equilibrated with buffer A without 1 mM DTT. The isolated complex was immediately mixed with DTT (1 mM), GroES, and denatured GFP in the presence or absence of BeFx (1 mM $BeCl_2$ and 10 mM NaF). GFP folding was initiated by the addition of a final concentration of 1 mM ATP. When BeFx was not included in the reaction mixture, the mixture of hexokinase (40 U/ml, final concentration) and glucose (50 mM, final concentration) was added to the mixture 3 sec after the addition of ATP to prevent the turnover of the functional GroE cycle [16, 34]. The final concentrations of

the proteins were 0.01 μM GFP, 0.12 μM WT-EL/ES bullet-shaped complex (or 0.3 μM ELΔC/ES complex), and 0.24 μM ES (or 0.6 μM ES), respectively. GFP folding was monitored by its fluorescence at 509 nm and then analyzed by gel-filtration chromatography as described above.

1-3. Results

1-3-1. Effects of C-terminal truncation on GFP encapsulation within the single-ring GroEL/GroES complex

The author first analyzed GFP folding mediated by a single-ring variant of GroEL (SR1) and GroES (ES). Acid-denatured GFP was diluted into the solution containing excess amounts of SR1 and ES, and refolding kinetics were monitored by the recovered fluorescence of GFP at 509 nm. A slight increase in fluorescence was observed just after mixing GFP with the excess amount of SR1/ES, indicating that the folding of GFP was largely arrested by the interaction with SR1. Arrested folding was resumed by the subsequent addition of ATP 200 sec after the initiation of the reaction. The folding reaction of GFP mediated by SR1/ES proceeded efficiently, and the yield of folding was similar to that of spontaneous folding in the absence of SR1 (Fig. 1-1A). Previous studies demonstrated that the kinetics of GFP folding mediated by GroE had an initial lag phase [35, 36]. The author also observed this lag phase in the initial kinetics of GroE-mediated GFP folding (data not shown); however, the author did not examine this kinetics in more detail in the present study.

To investigate the effects of C-terminal truncation on GFP folding mediated by SR1, the author constructed a C-terminal-truncated SR1 mutant (SR1ΔC), which lacked 23 amino acid residues at the C-terminus. Truncation was confirmed by SDS-PAGE, in which the C-terminal-truncated mutants migrated faster than full-length GroEL (data not shown). Although a slightly higher concentration of SR1ΔC was required for the efficient binding of denatured GFP than that of full-length SR1, the overall refolding kinetics of GFP were indistinguishable from those mediated by full-length SR1/ES (Fig. 1-1A).

The deletion of 23 residues in the C-terminal did not appear to affect the refolding kinetics of GFP when monitored by the recovery of fluorescence. The author then evaluated the yield of GFP that folded within the cage (encapsulation yield) during the process of refolding. The fluorescence intensity was almost saturated 25 min after the initiation of folding (the addition of ATP), and an aliquot of the reaction mixture was collected for gel-filtration chromatography with the Superdex-200 column. As previously demonstrated, the peak of encapsulated GFP within the SR1/ES cage was separate from that of free GFP [8, 37]. The author evaluated the encapsulation yield by the SR1/ES complex by comparing the areas of the two peaks. During the process of dilution of acid-denatured protein by the refolding buffer, a

significant amount of GFP molecules did not bind to GroEL. Since the unbound GFP refolded spontaneously and was eluted as free GFP in the gel-filtration analysis, the author eliminated its contribution using equation [1] (see Materials and Methods). The obtained encapsulation yield by the SR1/ES complex was 64.4 %, which was almost the same as that obtained by the SR1(D398A)/ES/ATPγS complex as shown in chapter 3 [37]. The author confirmed that the SR1/ES/GFP ternary complex was stable throughout the folding reaction, because the encapsulation yield of GFP was unchanged when the reaction mixture was reanalyzed after a 145-min incubation at 25°C (data not shown).

The same analysis was also performed for SR1ΔC, the C-terminal-truncated mutant of SR1, and the author found that the yield of in-cage folding was markedly decreased by C-terminal truncation (Fig. 1-1B and Table 1-1). This was in marked contrast to the results of the essentially same refolding kinetics monitored by GFP fluorescence. This demonstrated that the C-terminal region was essential for the efficient in-cage folding of GFP mediated by SR1. Although the yield of encapsulation by SR1ΔC/ES was much lower than that by SR1/ES, a significant amount of GFP was encapsulated and eluted as the SR1ΔC/ES/GFP ternary complex at 25 min. Importantly, once formed, the SR1ΔC/ES/GFP ternary complex was very stable for at least 2 hours even though it lacked C-terminal tails, as demonstrated by the gel-filtration analysis (Fig. 1-1C).

Table 1-1. The encapsulation yield of acid-denatured GFP by various GroEL mutants.

protein species	encapsulation efficiency (%)	corresponding figure
WT-EL (football)	79.0 ± 0.4	Figs. 1-3C, D
ELΔC (football)	86.0 ± 0.1	Figs. 1-3C, D
SR1	64.4 ± 0.8	Figs. 1-1A, B
SR1ΔC	15.2 ± 0.2	Figs. 1-1A, B
EL52/398 (football)	87.1 ± 0.8	Figs. 1-3A, B
EL52/398ΔC (football)	91.5 ± 0.8	Figs. 1-3A, B
SR52/398	68.1 ± 0.7	data not shown
SR52/398ΔC	18.9 ± 1.1	data not shown
WT-EL (bullet --> football)	74.4 ± 0.5	Figs. 1-4B, C
WT-EL (bullet --> bullet)	67.4 ± 0.2	Figs. 1-4B, C
ELΔC (bullet --> football)	86.2 ± 0.7	Figs. 1-4F, G
ELΔC (bullet --> bullet)	50.1 ± 0.4	Figs. 1-4F, G

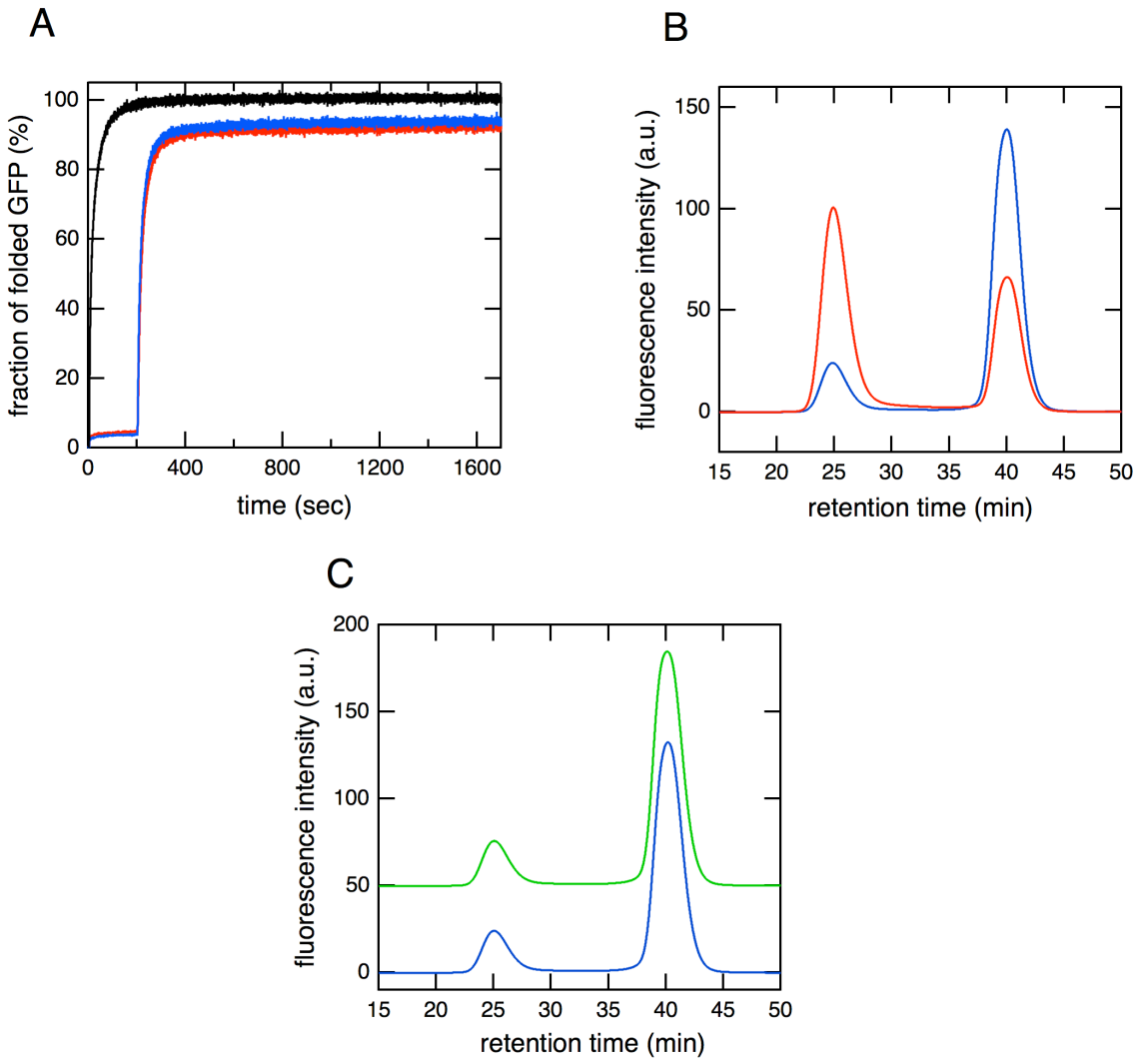

Fig. 1-1. Refolding kinetics of GFP mediated by single-ring variant SR1 and GroES. (A) Refolding kinetics of acid-denatured GFP monitored by fluorescence at 509 nm in the absence of SR1 and GroES (black), in the presence of 0.8 μM of SR1 and 1.6 μM of GroES (red), and in the presence of 2.0 μM of SR1ΔC and 4.0 μM of GroES (blue). In the red and blue traces, 2 mM of ATP was added 200 sec after this dilution of acid-denatured GFP by the refolding buffer, which contained SR1 (SR1ΔC) and GroES. (B) Size exclusion chromatography of refolded GFP in the presence of SR1 (red) or SR1ΔC (blue) and GroES was monitored by fluorescence at 509 nm. After monitoring the refolding kinetics by fluorescence (25 min after the addition of ATP), an aliquot of the mixture was subjected to chromatography. The yield of encapsulation without the contribution of spontaneous refolding was calculated by equation [1]. (C) The stability of the SR1ΔC/ES/GFP ternary complex. Twenty-five minutes (blue) or 145 min (green) after the addition of ATP to trigger refolding, the mixture was subjected to size exclusion chromatography.

1-3-2. Not folded, but denatured GFP escaped from the SR1ΔC-EL/GroES complex

The analysis by size-exclusion chromatography demonstrated that the 23 residues in the C-terminal were necessary for efficient encapsulation by SR1/ES during the refolding process of GFP. This result suggested that the GFP molecule easily escaped from the bottom pore of the SR1ΔC/ES chamber. On the other hand, the SR1ΔC/ES/GFP ternary complex was highly stable, as revealed by the gel-filtration analysis (Fig. 1-1C). This means that once GFP folded into its native state within the cage, it does not easily escape from the SR1ΔC/ES complex, even in the absence of the C-terminal region. In other words, the folding and escape of GFP from the SR1ΔC/ES chamber appeared to be competing with each other, and only a GFP molecule in a denatured conformation escaped through the large pore at the bottom of SR1ΔC/ES chamber. To demonstrate this hypothesis, the N265A mutant of GroEL (a substrate-trap mutant) was added to the reaction mixture. The substrate-trap mutant has been shown to bind a denatured protein more strongly than wild-type GroEL even in the presence of ATP, although it does not bind GroES [31, 38]. When an excess amount of the substrate-trap mutant was present in the refolding mixture of SR1ΔC/ES/GFP, the yield of GFP folding was markedly decreased (Fig. 1-2A). Furthermore, size-exclusion chromatography revealed that the intensity of the peak corresponding to free GFP at 39 min was significantly reduced, whereas that corresponding to the GFP co-eluted with SR1ΔC/ES at 25 min was not affected by the presence of the substrate-trap mutant (Fig. 1-2B). These results indicated that GFP escaped from the large pore at the bottom of the SR1ΔC/ES complex in a denatured conformation.

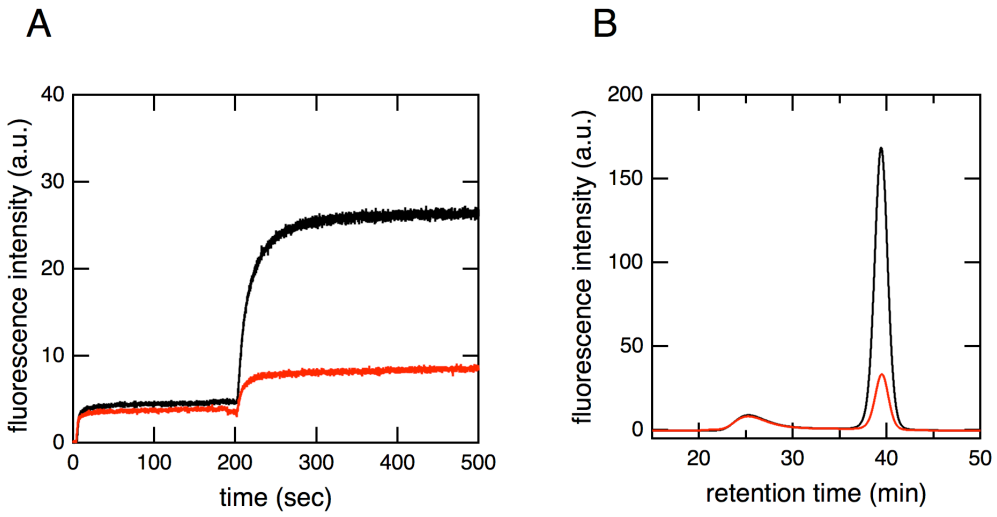

Fig. 1-2. Effects of a substrate-trap (N265A) mutant of GroEL on refolding kinetics of GFP mediated by SR1ΔC/ES. (A) The refolding kinetics of acid-denatured GFP monitored by fluorescence at 509 nm in the absence (black) and presence (red) of a substrate-trap mutant. Acid-denatured GFP was first diluted in the refolding buffer containing SR1ΔC and GroES, and ATP was added 200 sec after the initiation of the reaction. In the red trace, an excess amount of the substrate-trap mutant was added 10 sec before the addition of ATP. (B) Size exclusion chromatography of GFP refolding mixture in the absence (black) and presence (red) of a substrate-trap mutant. After monitoring the refolding kinetics for 500 sec by a fluorescence spectrophotometer, an aliquot of the refolding mixture was injected into the Superdex-200 HR 10/30 column (GE Healthcare).

1-3-3. GFP folding mediated by the double-ring football-shaped $GroEL_{14}/GroES_{14}$ complex

The author analyzed the effects of C-terminal truncation on in-cage GFP folding mediated by the double-ring EL_{14}/ES_{14} football-shaped complex. To prevent the multiple turnover of the functional cycle of GroEL, the author used GroEL variants (EL52/398) in which the key residues for the ATP-hydrolysis were doubly mutated to alanine (D52A, D398A). Previous studies reported that the D398A variant of GroEL formed a football-shaped complex, in which both sides of the GroEL rings was occupied by GroES, in an ATP-dependent manner [12, 25, 26]. The additional ATPase-deficient mutation, D52A, was introduced to enhance the stability of the football-shaped complex [15, 39]. The formation of the football-shaped complex was confirmed by transmission electron microscopy (data not shown). The author also confirmed that the $(EL52/398)_{14}/ES_{14}$ complex was sufficiently stable to retain GFP encapsulation for at least 150 min (data not shown).

The author analyzed the refolding kinetics of acid-denatured GFP by monitoring its fluorescence recovery. As was the case for fluorescence recovery mediated by the SR1/ES complex, only a small (~5%) increase in intensity was observed just after the addition of acid-denatured GFP, indicating that most molecules were prevented from refolding by interacting with EL52/398 (Fig. 1-3A). ATP was then added 200 sec after the initiation of the reaction to trigger the formation of a football-shaped $(EL52/398)_{14}/ES_{14}$ complex. The formation of a football-shaped complex resulted in a large increase in the intensity of fluorescence, indicating that the refolding of GFP was proceeding efficiently in the complex. The overall refolding kinetics mediated by the C-terminal-truncated mutant, EL52/398ΔC, were similar to those mediated by the C-terminal intact form, EL52/398. In addition, the analysis by size-exclusion chromatography revealed that the yield of in-cage folding was essentially the same regardless of the presence of 23 residues in the C-terminal (Fig. 1-3B). This result was markedly different from that obtained for the single-ring variant, SR1, in which truncation of the C-terminal tail resulted in a marked decrease in the encapsulation yield (Fig. 1-1B). These results suggested that the C-terminal tail of GroEL was not required for the efficient encapsulation of substrate proteins. However, it may act as a barrier that prevents the encapsulated substrate from transferring between chambers.

The author also examined the effects of C-terminal truncation on the yield of in-cage folding mediated by the $WT\text{-}EL_{14}/ES_{14}$ football-shaped complex (Fig. 1-3C, D). It has been reported that WT-EL formed a stable football-shaped complex in the presence of ATP and berrium fluoride (BeFx) [40, 41]. The encapsulation yield by the $WT\text{-}EL_{14}/ES_{14}$ football-shaped complex was slightly lower than that by the $(EL52/398)_{14}/ES_{14}$ complex (Table 1-1). It should be noted that C-terminal truncation also did not significantly affect the encapsulation yield by the $WT\text{-}EL_{14}/ES_{14}$ complex, as shown in Figure 1-3D.

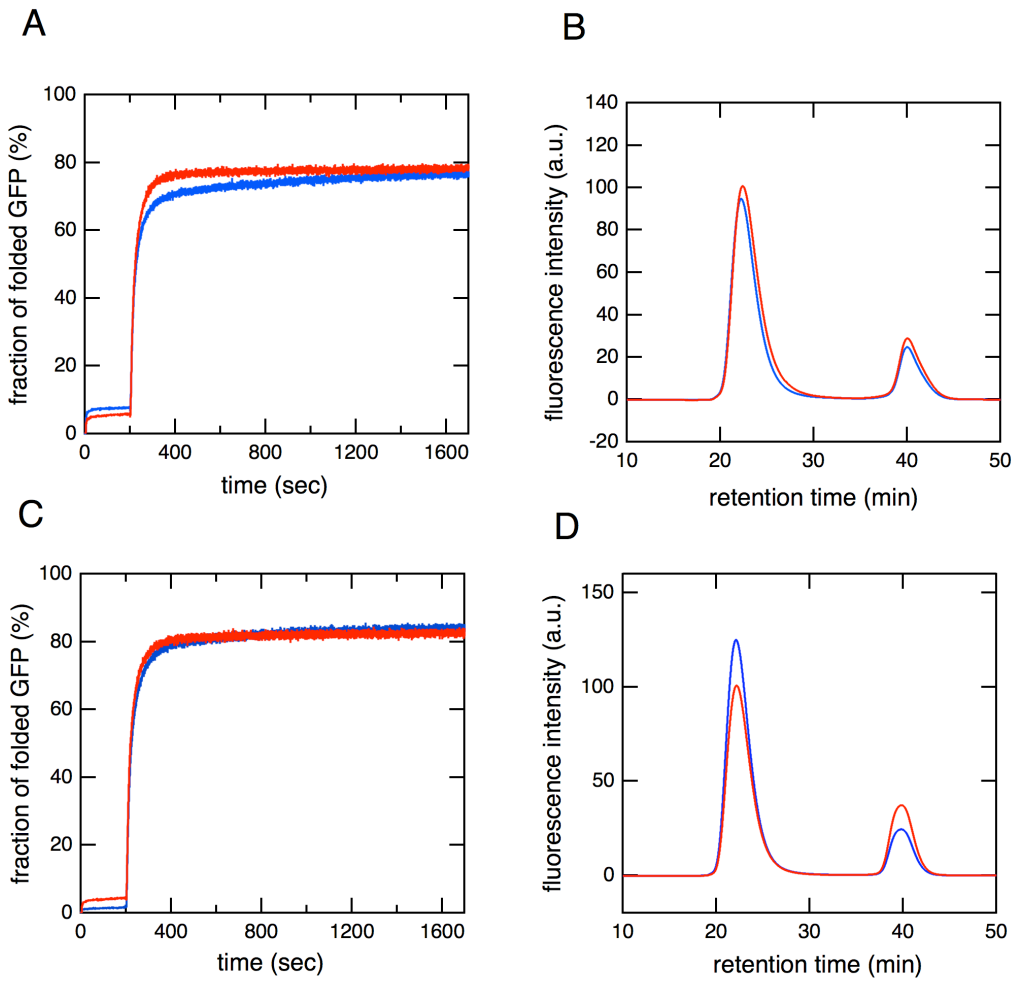

Fig. 1-3. Effects of the C-terminal truncation on refolding kinetics and encapsulation yield of GFP mediated by the $EL_{14}ES_{14}$ football-shaped complex. (A) The overall refolding kinetics of acid-denatured GFP. Acid-denatured GFP was diluted in refolding buffer, which contained EL52/398 (red) or EL52/398ΔC (blue) and GroES. An excess amount of ATP was added 200 sec after this dilution. (B) Size-exclusion chromatography of the refolded GFP mediated by the football-shaped complex of $(EL52/398)_{14}ES_{14}$ (red) or $(EL52/398\Delta C)_{14}ES_{14}$ (blue). (C) The refolding kinetics of acid-denatured GFP mediated by the football-shaped complex formed by WT-EL and BeFx. Acid-denatured GFP was diluted in refolding buffer, which contained WT-EL (red) or ELΔC (blue), GroES, and BeFx. An excess amount of ATP was added 200 sec after this dilution. (D) Size-exclusion chromatography of the refolded GFP mediated by the football-shaped complex of WT-$EL_{14}ES_{14}$ (red) or $EL\Delta C_{14}ES_{14}$ (blue), which was stably formed in the presence of BeFx.

1-3-4. Comparison of the encapsulation yield of GFP by bullet- and football-shaped complexes

Chen et al. [16] recently reported that the C-terminal truncation of the WT-EL/ES/ADP bullet-shaped complex resulted in a marked decrease in the encapsulation yield of acid-denatured GFP. Under their experimental conditions, the addition of ATP triggered the encapsulation of GFP within the newly formed *cis*-ring, whereas the GroES that had bound to the preformed *cis*-ring dissociated rapidly to form the bullet-shaped EL_{14}/ES_7 complex again at the opposite ring (Fig. 1-4A). On the other hand, the author herein revealed that the encapsulation yield by the WT-EL_{14}/ES_{14} football-shaped complex was not affected by C-terminal truncation. Therefore, the author assumed that the denatured GFP encapsulated within a newly formed *cis*-ring may travel to the *trans*-ring through a large pore at the bottom unless the C-terminal tails were present. The GFP molecule that translocated to the trans-ring could then easily escape to the bulk solution. To demonstrate this hypothesis, the author performed a similar experiment, in which the WT-EL_{14}/ES_7 bullet complex was first prepared in the presence of ADP, and acid-denatured GFP was added to form a stable GFP/EL_{14}/ES_7 *trans*-ternary complex. ATP was then added in the absence or presence of BeFx. In the absence of BeFx, the addition of ATP results in the binding of GroES to the ring that has not been occupied by another GroES, which dissociates simultaneously. This will lead to the formation of a bullet-shaped, GFP/EL_{14}/ES_7 *cis*-ternary complex (Fig. 1-4A, upper pathway). To prevent further ATP hydrolysis and conformational switching by GroEL, an excess amount of hexokinase was added 3 sec after the addition of ATP (see Materials and Methods). On the other hand, in the presence of BeFx, the addition of ATP does not trigger the dissociation of GroES from the complex, but results in the formation of a football-shaped complex (Fig. 1-4A, lower pathway).

The author analyzed the encapsulation yield of GFP mediated by a bullet- or a football-shaped complex using WT-EL, which has 23-residue C-terminal tails. The overall refolding kinetics of GFP monitored by the recovery of fluorescence was similar (Fig. 1-4B). In addition, size-exclusion chromatography revealed that the encapsulation yield was also similar between the bullet- and football-shaped complexes (Fig. 1-4C). The author then performed the same experiment using the ELΔC mutant, which lacks C-terminal tails. The formation of bullet- and football-shaped complexes by ELΔC was monitored by transmission electron microscopy. Similar to WT-EL, ELΔC also formed a bullet-shaped complex in the presence of ADP and BeFx, and a football-shaped complex in the presence of ATP and BeFx (Fig. 1-4D, E). The overall refolding kinetics monitored by the fluorescence of GFP was again similar (Fig. 1-4F). However, the encapsulation yield of the substrate by the bullet-shaped complex was markedly lower than that by the football-shaped complex (approximately 40%

less; Fig. 1-4G), which was consistent with previous findings. These results suggested that denatured GFP was able to translocate from the *cis*- to *trans*-ring through the bottom pore of the GroE cage unless the C-terminal tails were present.

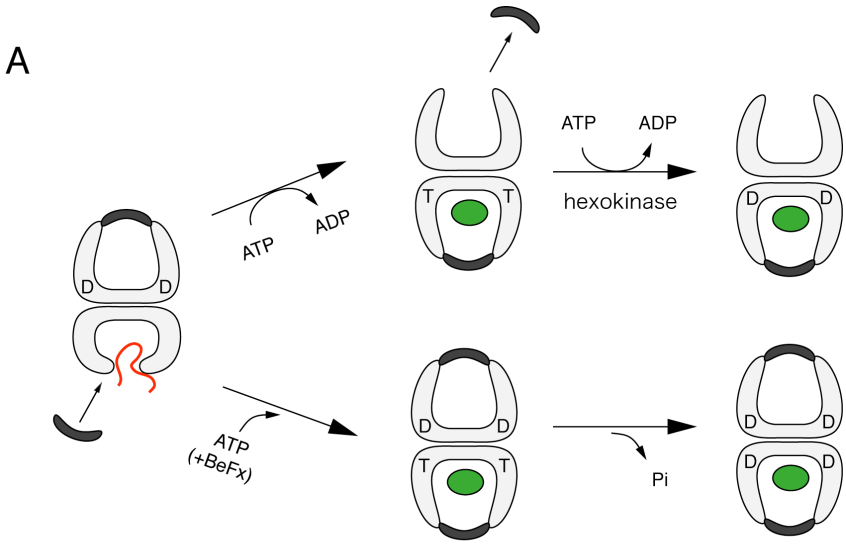

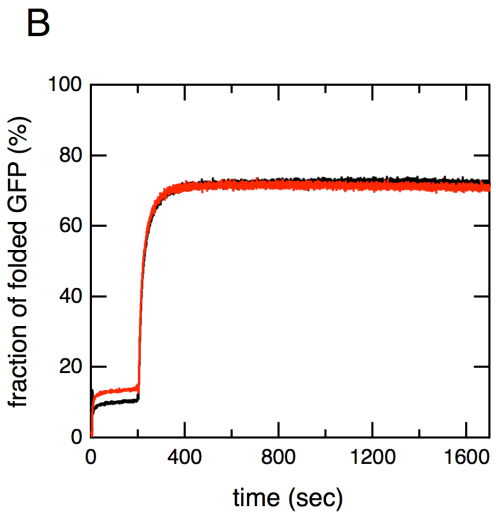

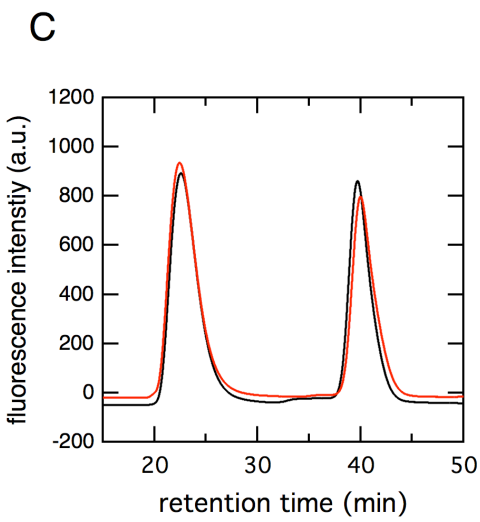

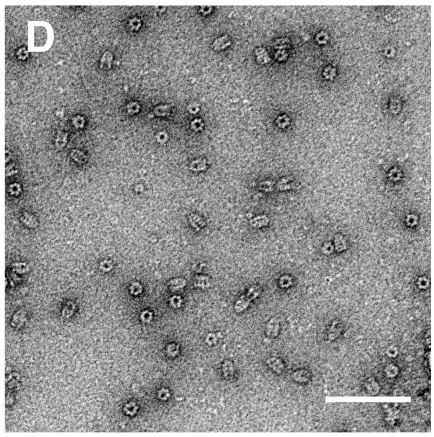

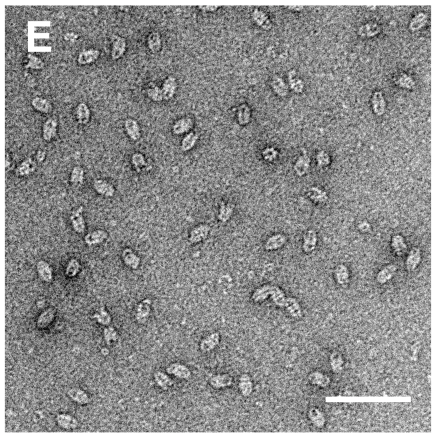

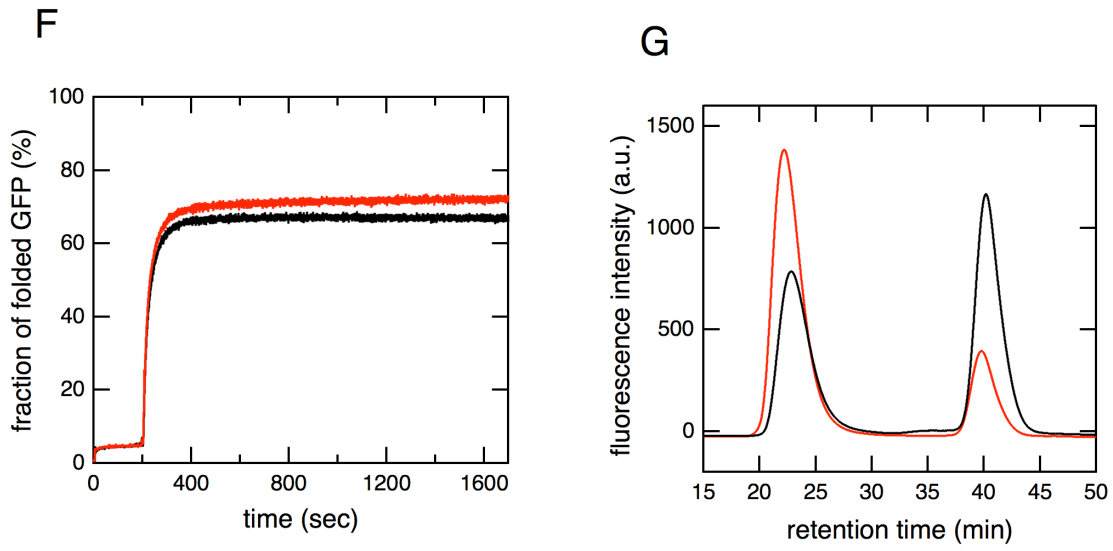

Fig. 1-4. The refolding of GFP by the $EL_{14}ES_7$ bullet-shaped complex versus the $EL_{14}ES_{14}$ football-shaped complex. (A) A schematic drawing of the experimental procedure. Acid-denatured GFP (indicated by a red string) was first captured on the *trans*-ring of the bullet-shaped $EL_{14}ES_7$ complex. The addition of an excess amount of ATP (upper pathway) triggered the binding of GroES and nucleotides, as well as the release of another GroES and ADP, which had bound to the opposite ring. This resulted in the formation of the $EL_{14}ES_7$GFP bullet-shaped *cis*-ternary complex. To prevent further ATP hydrolysis and conformational switching by GroEL, an excess amount of hexokinase was added. In the presence of BeFx (lower pathway), the dissociation of GroES and ADP was not triggered. This resulted in the formation of the $EL_{14}ES_{14}$GFP football-shaped ternary complex. (B) The refolding kinetics of acid-denatured GFP mediated by WT-EL and GroES. GFP was first diluted in refolding buffer, which contained WT-EL and GroES in the absence (black) and presence (red) of BeFx. An excess amount of ATP was added 200 sec after this dilution. In the black trace, hexokinase was added 3 sec after the addition of ATP. (C) Size-exclusion chromatography of refolded GFP mediated by the bullet-shaped WT-$EL_{14}ES_7$ complex (black) or football-shaped WT-$EL_{14}ES_{14}$ complex (red). (D) A transmission electron micrograph of the bullet-shaped $EL\Delta C_{14}ES_7$ complex formed in the presence of ADP and BeFx. (E) A transmission electron micrograph of the football-shaped $EL\Delta C_{14}ES_{14}$ complex formed in the presence of ATP and BeFx. (F) The refolding kinetics of acid-denatured GFP mediated by ELΔC and GroES. GFP was first diluted in the refolding buffer containing ELΔC and GroES in the absence (black) and presence (red) of BeFx. An excess amount of ATP was added 200 sec after this dilution. In the black trace, hexokinase was added 3 sec after the addition of ATP. (G) Size-exclusion chromatography of the refolded GFP mediated by bullet-shaped $EL\Delta C_{14}ES_7$ complex (black) or the football-shaped $EL\Delta C_{14}ES_{14}$ complex (red).

1-4. Discussion

The roles of the unstructured C-terminal tails of GroEL have been intensively studied both *in vitro* [16, 20, 22, 36, 42, 43] and *in vivo* [44-46]. Consequently, the C-terminal tails are now considered to be involved in many aspects of GroE functions. It has been reported that C-terminal truncation affected both the intra-ring positive-cooperativity and inter-ring negative-cooperativity in ATP hydrolysis, altering the turnover rate of the GroE cycle [22, 36, 42]. In addition, C-terminal-truncated GroEL failed to efficiently encapsulate several substrate proteins including GFP, which was also used in this study [16]. The partitioning of the C-terminal regions in the unfolding process has also been reported [42]. Importantly, C-terminal-truncated GroEL was unable to efficiently assist in the folding of rhodanase [22] or Rubisco [42], which are known to be stringent substrates. Therefore, understanding the multiple roles of the C-terminal tails is important for elucidating the mechanism underlying GroE-assisted protein folding.

In the present study, the author examined the effects of truncation of the flexible 23-residue at the C-terminal of GroEL on refolding kinetics and the yield of encapsulation of the substrate protein, GFP. A previous study revealed using cryo-electron microscopy that the C-terminal tails of GroEL interacted with the encapsulated substrate protein, Rubisco, suggesting that these tails directly participated in the substrate encapsulation process [16]. Interestingly, the author found that the effects of C-terminal truncation on the encapsulation yields by single- and double-ring GroEL were markedly different. In the case of the single-ring variant, SR1, the C-terminal regions appeared to be necessary for the efficient encapsulation of substrate proteins. However, this was revealed to be the result of the escape of the substrate protein in a denatured conformation through the large pore at the bottom of the GroEL ring. On the other hand, the double-ring EL_{14}/ES_{14} football complex was able to encapsulate GFP within the cage even in the absence of C-terminal tails as efficiently as full-length EL, indicating that the C-terminal regions were not necessarily required for efficient protein encapsulation.

One of the central questions regarding GroE functions is how GroE encapsulates the substrate protein within the cavity in spite of entropic difficulties. Weaver et al. [42] recently showed that denatured Rubisco, which bound to the apical domain of GroEL, was pulled down by the C-terminal tails toward the inner cavity. This interaction appears to contribute significantly to the encapsulation of substrate proteins. However, the encapsulation yield of the substrate protein, GFP, did not differ significantly in the presence and absence of C-terminal tails in the present study, indicating that it is not the major driving force for the encapsulation of the substrate protein, at least for GFP.

1-4-1. C-terminal tails blocked the escape of GFP through the bottom pore of the cavity

C-terminal truncation markedly reduced the encapsulation yield of GFP mediated by the single-ring $SR1_7/ES_7$ complex, whereas truncation did not affect the yield by the double-ring EL_{14}/ES_{14} football complex. These results were not attributed to differences in the stabilities of the complexes. As revealed by size-exclusion chromatography, both the single-ring $SR1_7/ES_7$/GFP and double-ring $(EL52/398)_{14}/ES_{14}$/GFP ternary complexes were very stable once they were formed. Thus, it was likely that the double-ring structure of GroEL was critical for efficient GFP encapsulation in the absence of the C-terminal tails. The author assumed that encapsulated GFP escaped through the bottom of the cavity within the SR1ΔC/ES complex because the crystal structure of the EL/ES complex, in which the C-terminal tails were not identified, had a large pore at the bottom. On the other hand, the double-ring EL_{14}/ES_{14} football complex was composed of two rings that were stacked back-to-back, and the opposite ring, which was also capped by GroES, prevented GFP from escaping outside of the chamber, even in the absence of C-terminal tails.

This was further supported by an experiment in which the encapsulation yield of the denatured GFP by the $ELΔC_{14}/ES_7$ bullet complex was compared with that mediated by the $ELΔC_{14}/ES_{14}$ football complex. The results obtained showed that the yield depended strongly on whether the opposite ring to the GFP-encapsulated ring was occupied with GroES, indicating that GFP was able to translocate between two rings in the absence of the C-terminal tails. Taken together, the author concluded that the C-terminal regions were essential for retention of the substrate within the cavity by blocking its escape from the bottom pore. This conclusion was consistent with those of previous studies, which suggested that C-terminal tails were acting as a wall separating the two rings at the bottom of the cavity [22-24].

1-4-2. Effects of C-terminal truncation on the encapsulation yield by the football complex

The author found that the encapsulation yield of GFP mediated by the $EL_{14}ES_{14}$ football complex was slightly increased by C-terminal truncation. This was evident by the comparison of the elution profiles of WT-$EL_{14}ES_{14}$ and $ELΔC_{14}ES_{14}$ that were formed directly from WT-EL_{14} and $ELΔC_{14}$ (Fig. 1-3D), as well as by the comparison of WT-$EL_{14}ES_{14}$ and $ELΔC_{14}ES_{14}$ that were formed via WT-$EL_{14}ES_7$ and $ELΔC_{14}ES_7$ (Fig. 1-4C and G, red lines). Because the pore at the bottom of GroEL is sealed by the other ring in these football shaped $EL_{14}ES_{14}$ complexes, the differences in the yield do not seem to be caused by the escape from once formed *cis*-ternary complex, but rather by the differences in the encapsulation yield itself. The yield of substrate encapsulation was previously shown to be dependent on the hydrophobicity of the inner cavity of the GroE cage. The hydrophobic fluorescence dye pyrene was attached to the residues located inside the cavity of GroEL, and enhanced the

encapsulation yield of rhodanese [47]. Therefore, the slight increase in the encapsulation yield by C-terminal truncation may have been caused by the deletion of hydrophilic sequences (KNDAAD) in the C-terminal tails. The importance of these sequences for the in-cage folding of rhodanese has also been reported previously [22].

1-4-3. Folding of GFP inside the cage competed with leakage through the bottom pore

Another important result in the present study was that GFP escaped the SR1ΔC/ES complex in a denatured conformation. This was confirmed by adding the N265A substrate-trap mutant, which binds substrate proteins in a denatured state more strongly than WT-EL, in the refolding mixture mediated by the SR1ΔC/ES complex. In the case of single-ring variants, the truncation of C-terminal tails resulted in a marked decrease in the encapsulation yield of GFP (~65% for SR1/ES and ~15% for SR1ΔC/ES, Table 1-1). Since the substrate-trap mutant only binds proteins in a denatured conformation, this result indicates GFP molecules escape through the large pore in the denatured conformation. This is also supported by a structural point of view. From the X-ray crystallographic structures, the size of a pore at the bottom in the SR1ΔC/ES complex is estimated to be approximately 40 Å, whereas a shorter diameter of GFP molecule to be 50 Å.

Since GFP molecules only escape through a pore if they are in denatured conformations, three-fourths of GFP molecules escaped before they folded into the native conformation. It should be noted that the folding of GFP, which proceeds in the order of seconds as shown in the spontaneous refolding kinetics in Figure 1-1A, was markedly faster than that of stringent substrates, which typically take several minutes [18, 22, 25]. Therefore, the encapsulation yields of stringent substrates, such as rhodanese and Rubisco, are expected to be affected more by the truncation of C-terminal tails. In contrast to expectation, a previous study reported that C-terminal truncation slightly decreased (approximately 10%) the encapsulation yield of Rubisco [16]. This finding indicates that other factors, such as an interaction with the inner wall of the GroEL cavity, may affect the rate of refolding and/or escape from the large pore at the bottom of chamber.

1-4-4. Can substrate proteins translocate through the bottom even in the presence of the C-terminal tails?

The present study suggested that GFP molecules escaped from a large pore at the bottom of the cavity if 23 residues in the C-terminal of GroEL were truncated. It is worth to consider whether the substrate protein within the cavity escapes through the bottom pore in the presence of the C-terminal tails. The author found the encapsulation yield of GFP by the SR1/ES complex (~65%) was lower than that of the WT-EL_{14}/ES_{14} football-shaped complex (~75%).

Given that the C-terminal tails are not structured, but highly flexible, the author assumed that denatured GFP escaped outside the SR1/ES complex through the bottom even in the presence of the C-terminal tails. On the other hand, the encapsulation yields by the WT-EL_{14}/ES_{14} football-shaped complex and WT-EL_{14}/ES_{7} bullet-shaped complex were similar to each other. Therefore, it is unlikely that the translocation of the substrate protein occured during the functional GroE cycle; however, substrate proteins smaller than GFP might be able to translocate between the two rings even in the presence of the C-terminal regions.

1-4-5. Efficient substrate encapsulation by GroE required both incorporation and retention

A recent study revealed that substrate protein encapsulation by GroE was not necessarily perfect [47]. In the present study, the author found that 10-20% of GFP molecules were not encapsulated even when the author used the WT-$EL_{14}ES_{14}$ football-shaped complex, in which the leakage of GFP through the bottom pore must be inhibited (Table 1-1), indicating that such a fraction of GFP molecules was not incorporated within the GroE cavity. Taken together with the effects of C-terminal truncation on the encapsulation yield by SR1 (Table 1-1), these results suggest that the process of substrate protein encapsulation has to be considered as two steps, (1) ejection of the denatured substrate into the cavity, and (2) retention of the substrate within the cavity. Regarding (1), the denatured substrates were found to escape through the interface between GroEL and GroES [47], while for (2), the author showed that the C-terminal tails played a critical role in shielding the bottom pore, blocking the escape of the denatured GFP. Further studies are required to clarify the significance of the C-terminal tails in the encapsulation of other substrates.

Chapter 2

Ring-exchange reaction of chaperonin GroEL probed by fluorescence resonance energy transfer.

Abstract

During the past 20 years, the functional GroE cycle has been intensively studied. Although the two rings of GroEL, which are stacking back-to-back each other, are structurally the same, there is a negative-cooperativity between the rings [48]. As a result, only one of the two rings binds GroES, and it has been believed that GroE assists protein folding by using two cages alternately as a folding chamber [10]. In the most established model at present, an asymmetric EL_{14}/ES_7 bullet-shaped complex plays a central role in the functional cycle of GroE. Although a symmetric EL_{14}/ES_{14} football-shaped complex has also been found, its physiological role was not clear [49-54]. Recent studies, however, have suggested that the football-shaped complex is also an important intermediate during the functional cycle of GroE. In this model, there are two pathways in the functional cycle of GroE, and the major intermediate is switched from the bullet- to football-shaped complex depending on the concentration of the denatured proteins [11-13]. Very recently, the crystal structure of an EL_{14}/ES_{14} football-shaped complex has been solved [15, 41]. Remarkably, the contact surface area between two GroEL rings of the football-shaped complex was found to be smaller than that of the bullet-shaped complex composed of EL_{14}/ES_7, indicating weaker ring-ring interactions in the football-shaped complex. Previous studies have also reported that a double-ring GroEL transiently splits to two single-rings at the equatorial plane, suggesting that some relationship might be present between the formation of the football-shaped complex and the ring-splitting reaction.

To this end, in the present study, the author has investigated the ring-exchange reaction of GroEL by using fluorescence resonance energy transfer (FRET) between two rings across the equatorial plane (inter-ring FRET). The GroEL molecules labeled by donor fluorescent dye were incubated with the acceptor-labeled GroEL under the various conditions. If double-ring GroEL molecules split transiently to two separate rings and then reassociate to the double-ring, it would be possible to form a mixed-ring GroEL, which consists of a donor-labeled ring and an accepter-labeled ring. The formation of the mixed-ring GroEL could be detected by the inter-ring FRET. When GroEL molecules labeled by donor- and acceptor- fluorescent dye were co-incubated in the presence of ADP and berrium fluoride (BeFx), in which an EL_{14}/ES_7 bullet-shaped complex was stably formed, there was no change in the fluorescence intensity, indicating that the exchange reaction did not occur. In contrast, when GroEL molecules labeled by two different fluorescent dyes were co-incubated in the presence of ATP and BeFx where

the EL_{14}/ES_{14} football-shaped complex was stably formed, the fluorescence intensity of the donor fluorophore was gradually decreased while the intensity of the acceptor fluorophore was increased. When we performed the same experiment by using a single-ring variant of GroEL (SR1), no significant change in the fluorescence intensity was observed even in the presence of ATP and BeFx, indicating that the observed FRET in double-ring GroEL was due to the exchange of two heptameric rings. In summary, it is concluded that double-ring GroEL transiently split into two single-rings only when GroEL formed the EL_{14}/ES_{14} football complex. Importantly, the ring-exchange reaction observed in the present study seems to be relevant to the physiologically functional cycle of GroE because the rate of the exchange was strongly dependent on the concentration of denatured protein. It is also suggested that the formation of the football-shaped complex is facilitated by the presence of denatured substrate proteins during the GroE cycle. It is therefore considered that the formation of a symmetric football-shaped complex facilitated by the denatured substrate proteins may lead to the transient splitting of the $EL_{14}ES_{14}$ double-ring to two separate single-rings during the physiologically functional ATP-dependent GroE cycle.

Chapter 3
Evaluating the stability of an SR398/GroES chaperonin complex

3-1. Introduction

Many GroEL variants have been characterized in order to elucidate the mechanism of GroEL/GroES-assisted protein folding. These include a single-ring variant of GroEL (SR1) with four point mutations at the equatorial domain, the D398A mutation in which ATPase activity is markedly decreased, and the combination of these mutations referred to as SR398 [17]. SR398 has been considered to bind GroES irreversibly because the dissociation of GroES from the *cis*-ring is triggered by ATP hydrolysis in the *cis*-ring and by the subsequent binding of ATP to the *trans*-ring, which is absent in SR398. In the present study, the author used green fluorescent protein (GFP) as a substrate to re-examine the stability of an SR398/GroES chaperonin complex with the ATP-analogue, ATPγS.

3-2. Materials and Methods

Materials

ATPγS was purchased from Roche Diagnostics. Cy3 maleimide mono-reactive dye pack was purchased from GE Healthcare. Other reagents were purchased from Nacalai Tesque.

Protein expression and purification

The expression plasmid of the ATPase-deficient variant of SR1 (SR398) was constructed by the QuickChange method, using pEL-SR1 as a template. The Expression and purification of SR398, GroES and GFP were performed as described in chapter 1.

Encapsulation of GFP into the SR398/GroES complex

The encapsulation of GFP into the SR398/GroES complex was performed as follows. GFP in 75 mM imidazole, 150 mM NaCl, and 25 mM sodium phosphate (pH 8.0) was denatured by adding HCl at a final concentration of 130 mM. Acid-denatured GFP was then diluted into buffer C (50 mM Tris-HCl (pH 7.8), 1 mM EDTA, 1 mM DTT), which contained an excess amount of SR398. An excess amount of GroES in buffer C was then added to the SR398/GFP binary complex, and the buffer of the mixtures was exchanged with buffer D (50 mM Tris-HCl (pH 7.8), 100 mM KCl, 10 mM $MgCl_2$, 1 mM DTT) using an Amicon Ultra (Millipore) membrane filter with a 50 kDa molecular weight cut off (MWCO). The addition of ATPγS at a final concentration of 2 mM triggered the encapsulation of GFP into the SR398/GroES complex. Final concentrations of the proteins were 15 μM GFP, 30 μM SR398,

and 90 μM GroES.

An excess amount of free ATPγS and GroES, which were present in the SR398/GroES/GFP ternary complex prepared as described above, were removed by a membrane filter of 100 kDa MWCO and successive dilution by ten times with buffer D. The concentration-dilution process was repeated four times. The isolated ternary complex by the repeated concentration-dilution process was analyzed immediately by gel filtration chromatography using a Superdex 200 column (GE Healthcare) equilibrated with 50 mM Tris-HCl (pH 7.8), 10 mM KCl, and 10 mM $MgCl_2$. In addition, the isolated complex was also analyzed after incubation for 32 hours at 37°C in the presence or absence of 2 mM ATPγS and AMPPNP. The elution of the ternary complex and free GFP was monitored by the absorption of GFP at 489 nm.

Evaluation of the stability of the SR398/GroES complex

The SR398/GroES binary complex was formed and isolated by the same protocols as described above, except that GFP was absent. The isolated binary complex was analyzed by the gel filtration chromatography monitored at 220 nm. The eluted peak fraction corresponding to the complex was collected and analyzed by SDS-PAGE. The SR398/Cy3-GroES binary complex was prepared by the same methods. The isolated complex was analyzed by gel filtration chromatography, monitoring the absorption of Cy3 dye at 552 nm. The stability of SR398/Cy3-GroES complex was evaluated by incubating with 10-fold excess amount of non-labeled GroES for 32 hours at 37°C in the presence or absence of 2 mM ATPγS.

Nucleotide exchange reaction

The nucleotide exchange was monitored as follows. The SR398/GroES binary complex formed in the presence of ATPγS was isolated as described above. The isolated complex was incubated for 32 hours at 37 °C in the presence of 2 mM AMPPNP. After the incubation, the excess amount of free AMPPNP was removed by repeated dilution-concentration process using a membrane filter of 100 kDa MWCO. The SR398/GroES/nucleotide complex was treated with $HClO_4$ at a final concentration of 1% to precipitate proteins. The aggregated proteins were removed by centrifugation at 20,000 g for 10 min. The supernatant was neutralized by adding 1.5 times volume of 500 mM Tris-HCl (pH 7.8), and then loaded onto Q-sepharose anion-exchange column equilibrated with 100 mM ammonium bicarbonate. The nucleotides were eluted by a linear gradient to 750 mM of ammonium bicarbonate while monitoring the absorption at 254 nm. Free ADP, AMPPNP and ATPγS were also analyzed by the same way.

3-3. Results

3-3-1. Formation of the SR398/GFP/GroES ternary complex

An acid-denatured green fluorescent protein (GFP) can bind effectively to GroEL [17]. Because of its specific fluorescence in the native state, GFP has been widely used to study chaperonin-mediated protein folding [8, 17, 69, 70]. A GFP variant with a stabilized F64L/S65T mutation was also trapped efficiently by SR398 during the course of refolding from an acid-denatured state. This was confirmed by size-exclusion chromatography (Fig. 3-1). After the addition of ATPγS and GroES to the SR398/GFP binary complex, the mixture was immediately subjected to gel filtration chromatography with the Superdex 200 column, monitored by the absorption of GFP at 489 nm. The elution profile showed two peaks at retention times of 25 min and 40 min. While the peak at 25 min corresponded to that of the SR398/GroES binary complex detected at 220 nm (see below, Fig. 3-3), the elution of free GFP was confirmed at 40 min. This result indicates that the peak at 25 min represented the SR398/GFP/GroES ternary complex. A comparison of the peak areas revealed that approximately 60% of bound GFP was encapsulated to form the SR398/GFP/GroES ternary complex.

The author examined the effect of an excess amount of free ATPγS and GroES on the stability of the ternary complex by removing them with a 100 kDa MWCO membrane filter. Whereas the molecular weight of the ternary complex (470 kDa) was markedly larger than the MWCO of the filter, free ATPγS, GroES (70 kDa), and GFP (27 kDa) passed through. The author found that four cycles of the concentration-dilution process by the filter effectively removed free GFP (Fig. 3-1B). This result suggests that the isolated ternary complex of SR398/GFP/GroES is stable at least for one hour during the concentration and dilution cycles.

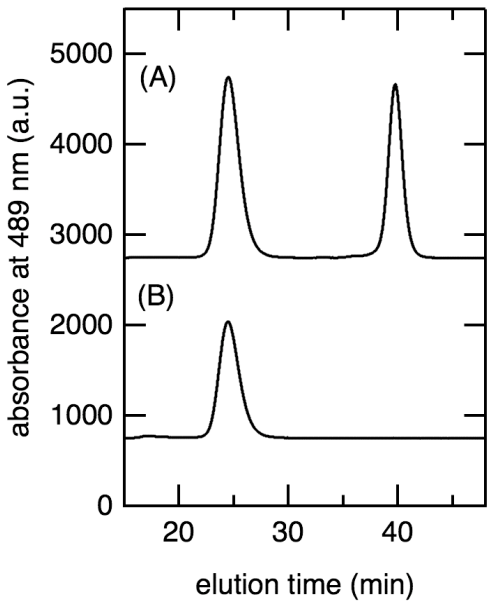

Fig. 3-1. Formation of the SR398/GFP/GroES ternary complex monitored by gel filtration chromatography. (A) Acid denatured GFP was mixed with SR398 and an excess amount of GroES and ATPγS was then added. While the peak at 25 min was assumed to the SR398/GFP/GroES ternary complex, the peak at 40 min corresponded to free GFP. (B) The mixture of the ternary complex, free GFP, and excess GroES and ATPγS was repeatedly concentrated and diluted with a 100 kDa MWCO membrane filter four times. The resulting isolated ternary complex was subjected to gel filtration chromatography. The peak at 40 min disappeared.

3-3-2. Stability of the SR398/GFP/GroES ternary complex

Because of the decrease in ATPase activity and lack of a *trans* ring, SR398 has been considered to bind GroES irreversibly. To ensure the stability of the SR398/GFP/GroES ternary complex, the author incubated the complex in the presence or absence of an excess amount of GroES and nucleotides. After various incubation times, the complex was subjected to size exclusion chromatography, monitored by the absorption of GFP at 489 nm. If the complex was adequately stable, GFP would co-elute with SR398 at 25 min.

The elution profile of the isolated complex on gel filtration chromatography showed a single peak at 25 min, monitored by the absorption of GFP at 489 nm (Fig. 3-2A). This elution profile was the same as that shown in Figure 3-1B. The author then incubated this ternary complex at 37°C for 32 hours. In contrast to the elution profile prior to the long incubation

period, the peak intensity at 25 min was markedly reduced and most GFP was eluted at 40 min (Fig. 3-2B). This result indicates that the ternary complex had dissociated during incubation. The author also incubated the isolated ternary complex under the same conditions, but in the presence of 2 mM ATPγS. In this case, most GFP eluted at 25 min, indicating that the ternary complex maintained binding during the long incubation period (Fig. 3-2C). These results demonstrate that the SR398/GroES complex was highly stable, only when an excess amount of free ATPγS was present. These results demonstrate that the ATPγS that bound to SR398 was stable for at least ~30 min. However, it slowly dissociates from SR398 during a longer 32 hour-incubation period unless an excess amount of free ATPγS is present. The rebinding of nucleotides to SR398 would occur in the presence of an excess amount of free ATPγS during the longer incubation period; therefore, GroES and GFP did not appear to dissociate from SR398. SR398 continued to bind and release ATPγS repeatedly while keeping GroES and GFP bound.

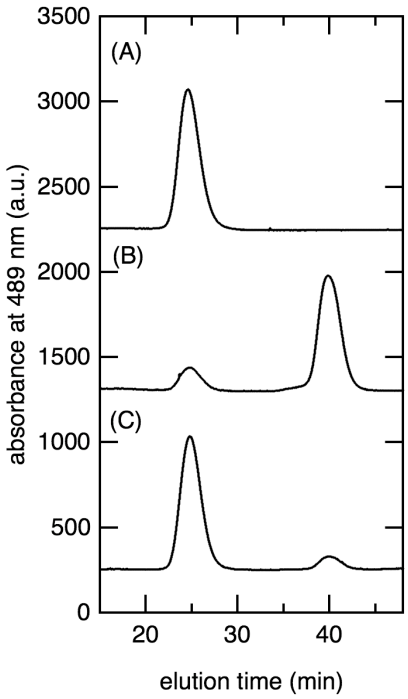

Fig. 3-2. Stability of the SR398/GFP/GroES ternary complex. The isolated ternary complex was subjected to gel filtration chromatography immediately after the concentration-dilution process (A), and after incubation for 32 hours at 37 °C in the absence of ATPγS (B), or in the presence of 2 mM ATPγS (C).

3-3-3. Stability of the SR398/GroES binary complex

The author also examined the stability of SR398/GroES binary complex by monitoring the absorption at 220 nm. The isolated SR398/GroES/ATPγS complex showed a single peak at 25 nm as previously observed by the GFP-specific absorbance at 489 nm (Fig. 3-3A). The isolated complex was incubated at 37 °C for 32 hours in the presence or absence of 2 mM ATPγS. After the incubation for 32 hour in the absence of ATPγS, a small but significant peak was appeared at 33 min (Fig. 3-3B). Because no such a peak was appeared when the complex was incubated with an excess amount of nucleotides (Fig. 3-3C), The author considered that the latter peak would be corresponding to the GroES that was dissociated from SR398. The author collected the peak at 25 min that had been incubated for 32 hours in the absence and presence of ATPγS. These fractions were concentrated and analyzed by SDS-PAGE (Fig. 3-3D). Contrarily to my expectation, the SDS-PAGE analysis revealed that as much as 70% of GroES was co-eluted with SR398 even in the absence of nucleotides. These results markedly different from those obtained by monitoring the GFP-specific absorbance at 489 nm (Fig. 3-2B, C).

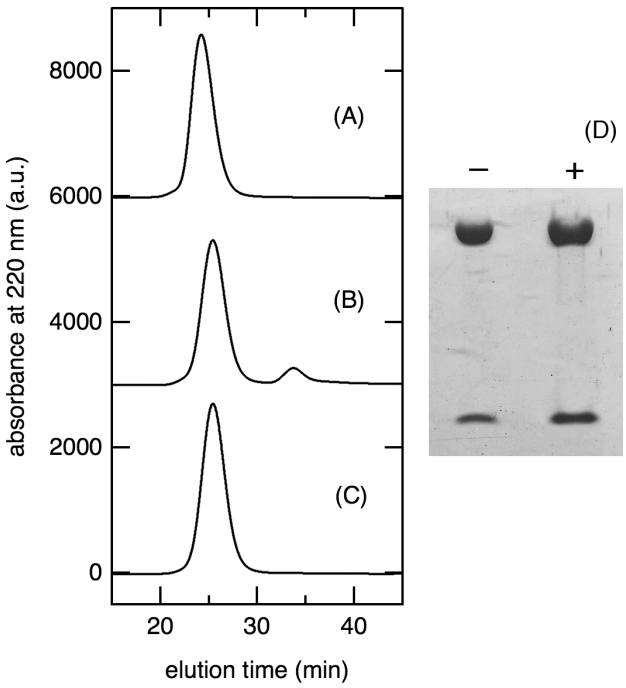

Fig. 3-3. Stability of the SR398/GroES binary complex. The isolated binary complex was subjected to gel filtration chromatography immediately after the concentration-dilution process (A), and after incubation for 32 hours at 37 °C in the absence of ATPγS (B), or in the presence of 2 mM ATPγS (C). SDS-PAGE analysis of binary complex eluted at 25 min after incubation in the absence (left lane) or presence of 2 mM ATPγS (right lane) (D).

3-3-4. Repeated binding and release of GroES from the SR398/GroES binary complex

The author considered the apparent difference in the stability of the complex monitored at 489 nm and 220 nm may be resulted from the re-association of GroES nucleotides to SR398 that was once dissociated from the complex. To demonstrate that such a repeated dissociation and re-association occurred during the incubation period, the author labeled Y71C-GroES by fluorescent dye Cy3-maleimide and incubated with 10-fold excess amount of non-labeled wild type GroES in the presence and absence of ATPγS. Immediately after the isolation of SR398/Cy3-GroES, only a single peak was eluted at 25 min (Fig. 3-4A). The complex was incubated at 37 °C for 32 hours with 10-fold excess amount of non-labeled GroES in the absence (Fig. 3-4B) or presence (Fig. 3-4C) of 2 mM ATPγS. In the absence of an excess amount of nucleotides, almost all the Cy3-GroES was dissociated from SR398 and eluted at 33 min. On the other hand, in the presence of ATPγS, as much as ~70% of Cy3-GroES was still bound to SR398 and co-eluted at 25 min. These results demonstrated that dissociation and re-association of GroES occurred in the absence of nucleotides, but dissociation GroES was significantly suppressed by an excess amount of nucleotides.

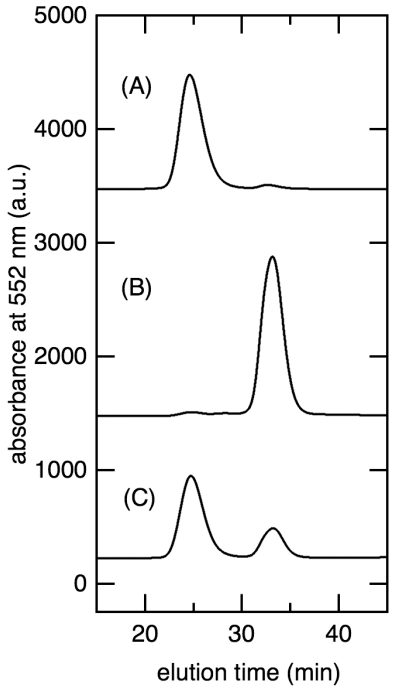

Fig. 3-4. Dissociation and re-association of GroES. The Y71C mutant of GroES was labeled by the fluorescence dye, Cy3 and formed a binary complex with SR398 in the presence of 2 mM of ATPγS. The binary complex was subjected to gel filtration chromatography immediately after the concentration-dilution process (A), indicating all the Cy3-labeled Y71C-GroES was co-eluted with SR398 at 25 min. The binary complex between SR398 and Cy3-labeled Y71C-GroES was co-incubated with 10-fold excess amount of non-labeled wild-type GroES for 32 hours at 37 °C in the absence of ATPγS (B), or in the presence of 2 mM ATPγS (C).

3-3-5. Nucleotide exchange reaction in the SR398/GroES binary complex

In contrast to the previous reports, the results presented here indicate that the non-hydrolyzable analogue of ATP, ATPγS, might dissociate and re-associate considerably to SR398/GroES complex. To demonstrate the nucleotide-exchange reaction proposed here, the author utilized another non-hydrolyzable analogue of ATP, AMPPNP. The author first confirmed that the excess amount of AMPPNP could also prevent the dissociation of GFP from SR398/GFP/GroES ternary complex that was stabilized by ATPγS (Fig. 3-5). The author also confirmed that the nucleotides ADP, ATPγS and AMPPNP were easily distinguished by the anion-exchange chromatography (Fig. 3-6). The author first prepared SR398/GroES binary complex in the presence of excess amount of ATPγS, and isolated the binary complex by

repeated concentration-dilution process. The isolated SR398/GroES/ATPγS complex was incubated at 37 °C for 0 and 32 hours in the presence of 2 mM AMPPNP. After the various time of incubation with AMPPNP, the SR398/GroES/nucleotide complex was purified again by repeated concentration-dilution process. Then the nucleotides were purified by precipitating proteins with 1 % of $HClO_4$, and analyzed by Q-sepharose anion-exchange chromatography (Fig. 3-7). Whereas only ATPγS was observed at 37 min immediately after the incubation with AMPPNP, almost all the nucleotides were exchanged with AMPPNP and eluted at 30 min after the incubation for 32 hours. The results demonstrated that the nucleotide-exchange reaction did occur during the incubation of SR398/GroES complex even though they were non-hydrolyzable analogues.

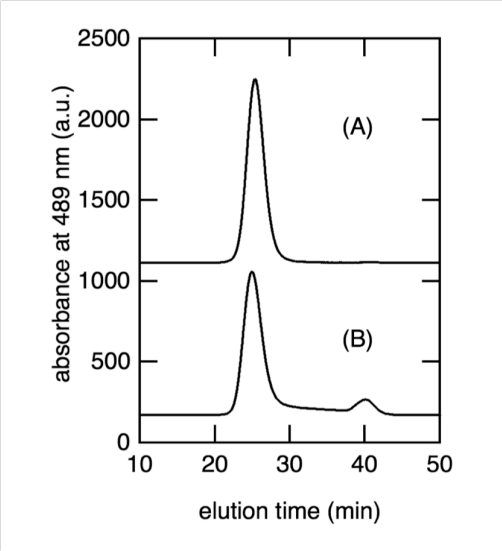

Fig. 3-5. Stability of the SR398/GroES/GFP ternary complex in the presence of an excess amount of free AMPPNP. The SR398/GroES/GFP ternary complex formed by ATPγS was isolated by the repeated concentration-dilution process, and incubated at 37 °C for 0 hour (A) and 32 hour (B) in the presence of 2 mM of AMPPNP.

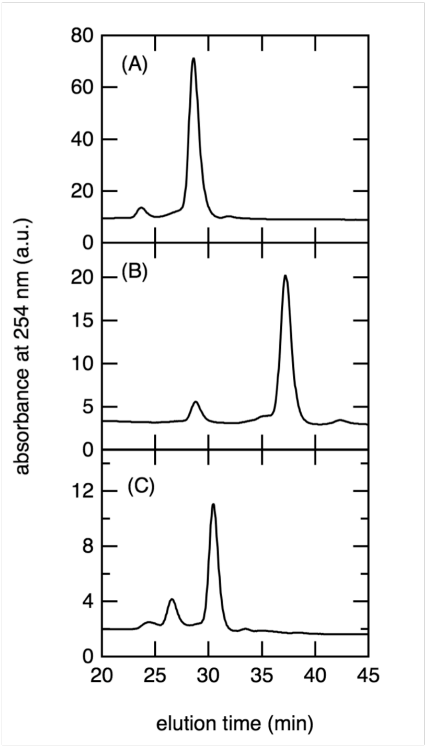

Fig. 3-6. Elution profile of each nucleotide analyzed by anion-exchange chromatography. ADP (A), ATPγS (B) and AMPPNP (C) were eluted with a linear gradient of ammonium bicarbonate, respectively.

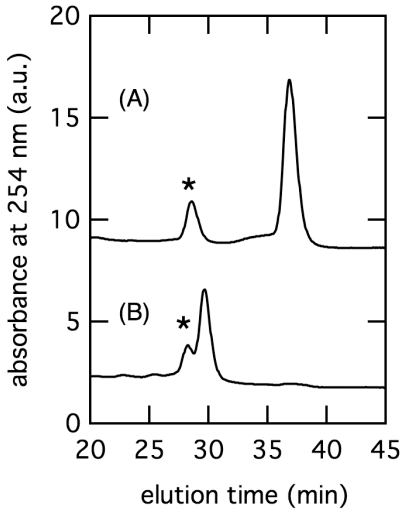

Fig. 3-7. Nucleotide-exchange reaction monitored by anion-exchange chromatography. The SR398/GroES binary complex formed by ATPγS was isolated by the repeated concentration-dilution process, and incubated at 37 °C for 0 hour (A) and 32 hour (B) in the presence of 2 mM of AMPPNP. The peaks at 29 min marked by the asterisks correspond to the ADP, which were produced by the hydrolysis of nucleotides during precipitation of proteins by $HClO_4$.

3-4. Discussion

3-4-1. Non-cooperative association/dissociation of ATPγS to/from SR398

Previous biochemical studies reported the positive cooperativity of ATP binding and hydrolysis between seven subunits in the same ring [48, 71]. In addition, a detailed comparison between the *trans*- and *cis*-ring of GroEL revealed that the ATP-binding site of GroEL become buried inside the molecule upon binding of GroES [9]. In the typical chaperonin cycle, GroEL-bound ATP does not exchange with free ATP until it is hydrolyzed to ADP. Nevertheless, my results indicated that non-hydrolyzable analogue ATPγS was exchanged with free ATPγS during a longer incubation period (Fig. 3-2B, C). This nucleotide exchange reaction is assumed to be markedly slower than that of the chaperonin reaction cycle because the SR398/GroES complex was stable during gel filtration chromatography even in the absence of free ATPγS (Fig. 3-2A). Therefore, the reaction may not be directly involved in the GroEL/GroES chaperonin cycle.

In contrast to ATP, ADP and ATP analogues have been shown to bind GroEL in a non-cooperative manner [71]. The dissociation of these nucleotides from GroEL is similarly considered to be non-cooperative. Therefore, the author observed apparent stable binding between SR398 and GroES in the presence of an excess amount of ATPγS. One or more nucleotides may dissociate from SR398 during the long incubation period for 32 hours; however, another ATPγS molecule re-associated to SR398 before all seven ATPγS and GroES dissociate from SR398. This has also been supported by the finding of Farr et al. [72], in which all seven subunits of GroEL were not required to bind GroES using tandem-fused GroEL. Wild-type GroEL stably binds GroES in up to 7 days in the presence of an excess amount of exchangeable ADP [34]. These results suggest that the cooperative dissociation of nucleotides from the *cis*-ring, which may be triggered by ATP binding to the *trans*-ring, is necessary for releasing GroES and substrates efficiently during the GroEL/GroES chaperonin cycle.

In conclusion, the author demonstrated that the stability of an SR398/GroES complex depends strongly on the presence of an excess amount of free ATP-analogues. In the absence of an excess amount of free ATPγS or AMPPNP, GFP that is encapsulated by SR398/GroES is slowly released to the bulk solution. On the other hand, the ternary complex of SR398/GFP/GroES appeared to be very stable for up to 32 hours in the presence of an excess amount of nucleotides. The author revealed that GroES also repeatedly associates to and dissociates from SR398 in the absence of an excess amount of nucleotides. This equilibrium was considerably shifted toward the association of SR398/GroES in the presence of nucleotides. Furthermore, the nucleotide exchange reaction was demonstrated by the anion exchange chromatography. These results indicate the presence of a non-cooperative exchange

reaction between SR398/GroES-bound nucleotides and bulk ligands, suggesting the importance of the cooperative dissociation of nucleotides from the *cis*-ring to release GroES and substrate proteins in the GroEL/GroES reaction cycle.

For the application of the EL/ES chaperonin cage to the nano carrier, it will be useful to use *Methanosarcina mazei* GroES, which binds GroEL more stably than *E.coli* GroES [2, 73], to enhance the stability of the cage.

Conclusion

In the present study, the author investigated the reaction mechanisms of GroE by the structural and physicochemical points of view. In chapter 1, the role of the C-terminal tails of GroEL in substrate protein encapsulation was elucidated. The author found that the C-terminal regions functioned as a barrier between the two rings. In the absence of the C-terminal tails, the encapsulated GFP escaped from the GroE cage through the bottom pore in the denatured state. These findings shed light on the previously unknown function of flexible C-terminal tails of GroEL.

In chapter 2, the author investigated the transient ring-splitting reaction by using inter-ring FRET. It was revealed that GroEL transiently split into single rings only when GroEL formed the symmetric football-shaped complex. Importantly, the rate of the ring-exchange reaction was accelerated depending on the concentration of the denatured protein. These findings suggest that the splitting of football-shaped complex should also occur in the functional ATPase cycle of GroE. The same reaction could be involved in the reaction cycle of GroE *in vivo*.

In chapter 3, the stability of an SR398/GroES complex was analyzed. It was demonstrated that the complex was extremely stable only in the presence of an excess amount of free nucleotides, suggesting that the nucleotides repeatedly associated to and dissociated from the complex in a non-cooperative manner. Remarkably, this nucleotide exchange reaction did not trigger the dissociation of GroES, suggesting that the cooperative dissociation of nucleotides from the *cis*-ring of the GroEL/GroES complex was important for the release of GroES and substrate proteins during the reaction cycle of GroE.

In conclusion, this study provided several important findings to elucidate the functional cycle of chaperonin GroE. All of these findings will be of great significance for the understanding of the mechanism of GroE-assisted protein folding.

Acknowledgements

The author would like to express his sincere gratitude to Professor Katsumi Matsuzaki (Graduate School of Pharmaceutical Sciences, Kyoto University) and Associate Professor Masaru Hoshino (Graduate School of Pharmaceutical Sciences, Kyoto University) for giving constant advices throughout this study. The author is also grateful to Assistant Professor Yoshiaki Yano (Graduate School of Pharmaceutical Sciences, Kyoto University) and Assistant Professor Kenichi Kawano (Graduate School of Pharmaceutical Sciences, Kyoto University) for their helpful discussions and advices.

The author is obliged to Professor Yasushi Kawata (Tottori University) for kind gift of a plasmid encoding GroE gene.

The author would like to express appreciation to Professor Hideki Taguchi (Tokyo Institute of Technology) for providing a helpful advice for the GroEL mutant.

The author would like to thank Professor Kenichi Namba (Osaka University) and Naoko Kajimura (Osaka University) for technical supports on TEM measurements.

The author is also grateful to the members of the Department of Biophysical Chemistry, Graduate School of Pharmaceutical Sciences, Kyoto University.

Finally, the author deeply thanks to his parents, brother, grandparents and relatives.

References

[1] Horwich, A.L., Low, K.B., Fenton, W.A., Hirshfield, I.N., and Furtak, K. (1993) Folding in vivo of bacterial cytoplasmic proteins: role of GroEL. *Cell* **74**, 909–917.

[2] Kerner, M.J., Naylor, D.J., Ishihama, Y., Maier, T., Chang, H.C., Stines, A.P., Georgopoulos, C., Frishman, D., Hayer-Hartl, M., Mann, M., Hartl, F.U. (2005) Proteome-wide analysis of chaperonin-dependent protein folding in Escherichia coli. *Cell* **122**, 209–220.

[3] Fujiwara, K., Ishihama, Y., Nakahigashi, K., Soga, T., Taguchi, H. (2010) A systematic survey of in vivo obligate chaperonin-dependent substrates. *EMBO J.* **29**, 1552–1564.

[4] Gething, M.J., and Sambrook, J. (1992) Protein folding in the cell. *Nature* **355**, 33–45.

[5] Horwich, A.L., Low, K.B., Fenton, W.A., Hirshfield, I.N., and Furtak, K. (1993) Folding in vivo of bacterial cytoplasmic proteins: role of GroEL. *Cell* **74**, 909–917.

[6] Braig, K., Otwinowski, Z., Hegde, R., Boisvert, D.C., Joachimiak, A., Horwich, A.L., and Sigler, P.B. (1994) The crystal structure of the bacterial chaperonin GroEL at 2.8 A. *Nature* **371**, 578–586.

[7] Hunt, J.F., Weaver, A.J., Landry, S.J., Gierasch, L., and Deisenhofer, J. (1996) The crystal structure of the GroES co-chaperonin at 2.8 A resolution. *Nature* **379**, 37–45.

[8] Weissman, J.S., Rye, H.S., Fenton, W.A., Beechem, J.M., and Horwich, A.L. (1996) Characterization of the active intermediate of a GroEL-GroES-mediated protein folding reaction. *Cell* **84**, 481–490.

[9] Xu, Z., Horwich, A.L., and Sigler, P.B. (1997) The crystal structure of the asymmetric GroEL-GroES-$(ADP)_7$ chaperonin complex. *Nature* **388**, 741–750.

[10] Horwich, A.L. (2011) Protein folding in the cell: an inside story. *Nat. Med.* **17**, 1211-6.

[11] Sameshima, T., Iizuka, R., Ueno, T., Funatsu, T. (2010) Denatured proteins facilitate the formation of the football-shaped GroEL-(GroES)2 complex. *Biochem. J.* **427**, 247-54.

[12] Yang, D., Ye, X., Lorimer, G.H. (2013) Symmetric GroEL:GroES2 complexes are the protein-folding functional form of the chaperonin nanomachine. *Proc. Natl. Acad. Sci. U S A.* **110**, 4298-305.

[13] Ye, X., Lorimer, G.H. (2013) Substrate protein switches GroE chaperonins from asymmetric to symmetric cycling by catalyzing nucleotide exchange. *Proc. Natl. Acad. Sci. U S A.* **110**, 4289-97.

[14] Taguchi, H., Amada, K., Murai, N., Yamakoshi, M., Yoshida, M. (1998) ATP-, K+-dependent heptamer exchange reaction produces hybrids between GroEL and chaperonin from Thermus thermophilus. *J. Biol. Chem.* **272**, 18155-60.

[15] Koike-Takeshita, A., Arakawa, T., Taguchi, H., Shimamura, T. (2014) Crystal structure of a symmetric football-shaped GroEL:GroES2-ATP14 complex determined at 3.8Å reveals rearrangement between two GroEL rings. *J. Mol. Biol.* **426**, 3634-41.

[16] Chen D.H., Madan D., Weaver J., Lin Z., Schröder G. F., Chiu W., Rye H. S. (2013) Visualizing GroEL/ES in the act of encapsulating a folding protein. *Cell* **153**, 1354–1365.

[17] Rye, H.S., Burston, S.G., Fenton, W.A., Beechem, J.M., Xu, Z., Sigler, P.B., and Horwich, A.L. (1997) Distinct actions of cis and trans ATP within the double ring of the chaperonin GroEL. *Nature* **388**, 792–798.

[18] Apetri, A.C., Horwich, A.L. (2008) Chaperonin chamber accelerates protein folding through passive action of preventing aggregation. *Proc. Natl. Acad. Sci. U S A.* **105**, 17351-5.

[19] Horwich, A.L., Apetri, A.C., Fenton, W.A. (2009) The GroEL/GroES cis cavity as a passive anti-aggregation device. *FEBS Lett.* **583**, 2654-62.

[20] Tang, Y.C., Chang, H.C., Roeben, A., Wischnewski, D., Wischnewski, N., Kerner, M.J., Hartl, F.U., Hayer-Hartl, M. (2006) Structural features of the GroEL-GroES nano-cage required for rapid folding of encapsulated protein. *Cell* **125**, 903-14.

[21] Gupta, A.J., Haldar, S., Miličić, G., Hartl, F.U., Hayer-Hartl, M. (2014) Active cage mechanism of chaperonin-assisted protein folding demonstrated at single-molecule level. *J. Mol. Biol.* **426**, 2739-54.

[22] Machida K., Kono-Okada A., Hongo K., Mizobata T., Kawata Y. (2008) Hydrophilic residues ^{526}KNDAAD^{531} in the flexible C-terminal region of the chaperonin GroEL are critical for substrate protein folding within the central cavity. *J. Biol. Chem.* **283**, 6886–6896.

[23] Chen, S, Roseman, A.M., Hunter, A.S., Wood, S.P., Burston, S.G., Ranson, N.A., Clarke, A.R., Saibil, H.R. (1994) Location of a folding protein and shape changes in GroEL-GroES complexes imaged by cryo-electron microscopy. *Nature* **371**, 261-4.

[24] Thiyagarajan, P., Henderson, S.J., Joachimiak, A. (1996) Solution structures of GroEL and its complex with rhodanese from small-angle neutron scattering. *Structure* **4**, 79-88.

[25] Koike-Takeshita, A., Yoshida, M., Taguchi, H. (2008) Revisiting the GroEL-GroES reaction cycle via the symmetric intermediate implied by novel aspects of the GroEL(D398A) mutant. *J. Biol. Chem.* **283**, 23774-81.

[26] Sameshima, T., Ueno, T., Iizuka, R., Ishii, N., Terada, N., Okabe, K., Funatsu, T. (2008) Football- and bullet-shaped GroEL-GroES complexes coexist during the reaction cycle. *J. Biol. Chem.* **283**, 23765-73.

[27] Kawata, Y., Kawagoe, M., Hongo, K., Miyazaki, T., Higurashi, T., Mizobata, T., and Nagai, J. (1999) Functional communications between the apical and equatorial domains of GroEL through the intermediate domain. *Biochemistry* **38**, 15731–15740.

[28] Doering, D.S., and Matsudaira, P. (1996) Cysteine scanning mutagenesis at 40 of 76 positions in villin headpiece maps the F-actin binding site and structural features of the domain. *Biochemistry* **35**, 12677-12685.

[29] Weissman, J.S., Hohl, C.M., Kovalenko, O., Kashi, Y., Chen, S., Braig, K., Saibil, H.R., Fenton, W.A., Horwich, A.L. (1995) Mechanism of GroEL Action: Productive Release of Polypeptide from a Sequestered Position under GroES. *Cell* **83,** 577–587.

[30] Tanaka, S., Kawata, Y., Otting, G., Dixon, N.E., Matsuzaki, K., and Hoshino, M. (2010) Chaperonin-encapsulation of proteins for NMR. *Biochim. Biophys. Acta* **1804**, 866–871.

[31] Motojima, F., Makio, T., Aoki, K., Makino, Y., Kuwajima, K., and Yoshida, M. (2000) Hydrophilic residues at the apical domain of GroEL contribute to GroES binding but attenuate polypeptide binding. *Biochem. Biophys. Res. Commun.* **267**, 842–849.

[32] Higurashi, T., Hiragi, Y., Ichimura, K., Seki, Y., Soda, K., Mizobata, T., and Kawata, Y. (2003) Structural stability and solution structure of chaperonin GroES heptamer studied by synchrotron small-angle X-ray scattering. *J. Mol. Biol.* **333**, 605–620.

[33] Miller, W.G., and Lindow, S.E. (1997) An improved GFP cloning cassette designed for prokaryotic transcriptional fusions. *Gene* **191**, 149–153.

[34] Motojima, F., and Yoshida, M. (2003) Discrimination of ATP, ADP, and AMPPNP by chaperonin GroEL: hexokinase treatment revealed the exclusive role of ATP. *J. Biol. Chem.* **278**, 26648–26654.

[35] Ueno, T., Taguchi, H., Tadakuma, H., Yoshida, M., Funatsu, T. (2004) GroEL mediates protein folding with a two successive timer mechanism. *Mol. Cell.* **14**, 423-34.

[36] Suzuki M., Ueno T., Iizuka R., Miura T., Zako T., Akahori R., Miyake T., Shimamoto N., Aoki M., Tanii T., Ohdomari I., Funatsu T. (2008) Effect of the C-terminal truncation on the functional cycle of chaperonin GroEL: implication that the C-terminal region facilitates the transition from the folding-arrested to the folding-competent state. *J. Biol. Chem.* **283**, 23931–23939.

[37] Ishino, S., Kawata, Y., Ikegami, T., Matsuzaki, K. and Hoshino, M. (2014) Evaluation of the stability of an SR398/GroES chaperonin complex. *J. Biochem.* **155**, 295-300.

[38] Nojima, T., Murayama, S., Yoshida, M., Motojima, F. (2008) Determination of the number of active GroES subunits in the fused heptamer GroES required for interactions with GroEL. *J. Biol. Chem.* **283**, 18385-92.

[39] Koike-Takeshita, A., Mitsuoka, K., Taguchi, H. (2014) Asp-52 in Combination with Asp-398 Plays a Critical Role in ATP Hydrolysis of Chaperonin GroEL. *J. Biol. Chem.* **289**, 30005-11.

[40] Taguchi, H., Tsukuda, K., Motojima, F., Koike-Takeshita, A., Yoshida, M. (2004) BeF(x) stops the chaperonin cycle of GroEL-GroES and generates a complex with double folding chambers. *J. Biol. Chem.* **279**, 45737-43.

[41] Fei, X., Ye, X., LaRonde, N.A., Lorimer, G.H. (2014) Formation and structures of GroEL:GroES2 chaperonin footballs, the protein-folding functional form. *Proc. Natl. Acad. Sci. U S A.* **111**, 12775-80.

[42] Weaver, J., Rye, H.S. (2014) The C-terminal tails of the bacterial chaperonin GroEL stimulate protein folding by directly altering the conformation of a substrate protein. *J. Biol. Chem.* **289**, 23219-32.

[43] Farr, G.W., Fenton, W.A., Horwich, A.L. (2007) Perturbed ATPase activity and not "close confinement" of substrate in the cis cavity affects rates of folding by tail-multiplied GroEL. Proc. Natl. Acad. Sci. U S A. 104, 5342-7.

[44] McLennan, N.F., Girshovich, A.S., Lissin, N.M., Charters, Y., Masters, M. (1993) The strongly conserved carboxyl-terminus glycine-methionine motif of the Escherichia coli GroEL chaperonin is dispensable. Mol. Microbiol. **7**, 49-58.

[45] McLennan, N.F., McAteer, S., Masters, M. (1994) The tail of a chaperonin: the C-terminal region of Escherichia coli GroEL protein. Mol. Microbiol. **14**, 309-21.

[46] Burnett, B.P., Horwich, A.L., Low, K.B. (1994) A carboxy-terminal deletion impairs the assembly of GroEL and confers a pleiotropic phenotype in Escherichia coli K-12. J. Bacteriol. **176**, 6980-5.

[47] Motojima, F., Yoshida, M. (2010) Polypeptide in the chaperonin cage partly protrudes out and then folds inside or escapes outside. *EMBO J.* **29**, 4008-19.

[48] Yifrach, O., and Horovitz, A. (1995) Nested cooperativity in the ATPase activity of the oligomeric chaperonin GroEL. *Biochemistry* **34**, 5303–5308.

[49] Engel, A., Hayer-Hartl, M.K., Goldie, K.N., Pfeifer, G., Hegerl, R., Müller, S., da Silva, A.C., Baumeister, W., Hartl, F.U. (1995) Functional significance of symmetrical versus asymmetrical GroEL-GroES chaperonin complexes. *Science*. **269**, 832-6.

[50] Schmidt, M., Rutkat, K., Rachel, R., Pfeifer, G., Jaenicke, R., Viitanen, P., Lorimer, G., Buchner, J. (1994) Symmetric complexes of GroE chaperonins as part of the

functional cycle. *Science*. **265**, 656-9.

[51] Azem, A., Diamant, S., Kessel, M., Weiss, C., Goloubinoff, P. (1995) The protein-folding activity of chaperonins correlates with the symmetric GroEL14(GroES7)2 heterooligomer. *Proc. Natl. Acad. Sci. U S A*. **92**, 12021-5.

[52] Llorca, O., Marco, S., Carrascosa, J.L., Valpuesta, J.M. (1994) The formation of symmetrical GroEL-GroES complexes in the presence of ATP. *FEBS Lett*. **345**, 181-6.

[53] Llorca, O., Marco, S., Carrascosa, J.L., Valpuesta, J.M. (1997) Symmetric GroEL-GroES complexes can contain substrate simultaneously in both GroEL rings. *FEBS Lett*. **405**, 195-9.

[54] Sparrer, H., Rutkat, K., Buchner, J. (1997) Catalysis of protein folding by symmetric chaperone complexes. *Proc. Natl. Acad. Sci. U S A*. **94**, 1096-100.

[55] Shiseki, K., Murai, N., Motojima, F., Hisabori, T., Yoshida, M., Taguchi, H. (2001) Synchronized domain-opening motion of GroEL is essential for communication between the two rings. *J. Biol. Chem*. **276**, 11335-8.

[56] Yifrach, O., Horovitz, A. (1996) Allosteric control by ATP of non-folded protein binding to GroEL. *J. Mol. Biol*. **255**, 356-61.

[57] Okazaki, A., Ikura, T., Nikaido, K., Kuwajima, K. (1994) The chaperonin GroEL does not recognize apo-alpha-lactalbumin in the molten globule state. *Nat. Struct. Biol*. **1**,439-46.

[58] Sirur, A., Best, R.B. (2013) Effects of interactions with the GroEL cavity on protein folding rates. *Biophys. J*. **104**, 1098-106.

[59] Ishii, N., Taguchi, H., Sasabe, H., Yoshida, M. (1995) Equatorial split of holo-chaperonin from Thermus thermophilus by ATP and K+. *FEBS Lett*. **362**, 121-5.

[60] Viitanen, P.V., Lorimer, G.H., Seetharam, R., Gupta, R.S., Oppenheim, J., Thomas, J.O., Cowan, N.J. (1992) Mammalian mitochondrial chaperonin 60 functions as a single toroidal ring. *J. Biol. Chem*. **267**, 695-8.

[61] Truscott, K.N., Høj, P.B., Scopes, R.K. (1994) Purification and characterization of chaperonin 60 and chaperonin 10 from the anaerobic thermophile Thermoanaerobacter brockii. *Eur. J. Biochem*. **222**, 277-84.

[62] Todd, M.J., Walke, S., Lorimer, G., Truscott, K., Scopes, R.K. (1995) The single-ring Thermoanaerobacter brockii chaperonin 60 (Tbr-EL7) dimerizes to Tbr-EL14.Tbr-ES7 under protein folding conditions. *Biochemistry*. **34**, 14932-41.

[63] Burston, S.G., Weissman, J.S., Farr, G.W., Fenton, W.A., Horwich, A.L. (1996) Release of both native and non-native proteins from a cis-only GroEL ternary complex. *Nature*. **383**, 96-9.

[64] Llorca, O., Galán, A., Carrascosa, J.L., Muga, A., Valpuesta, J.M. (1998) GroEL under heat-shock. Switching from a folding to a storing function. *J. Biol. Chem.* **273**, 32587-94.

[65] Grason, J.P., Gresham, J.S., Widjaja, L., Wehri, S.C., Lorimer, G.H. (2008) Setting the chaperonin timer: the effects of K+ and substrate protein on ATP hydrolysis. *Proc. Natl. Acad. Sci. U S A.* **105**, 17334-8.

[66] Shabala, L., Bowman, J., Brown, J., Ross, T., McMeekin, T., Shabala, S. (2009) Ion transport and osmotic adjustment in Escherichia coli in response to ionic and non-ionic osmotica. *Environ. Microbiol.* **11**, 137-48.

[67] Inobe, T., Kikushima, K., Makio, T., Arai, M., Kuwajima, K. (2003) The allosteric transition of GroEL induced by metal fluoride-ADP complexes. *J. Mol. Biol.* **329**, 121-34.

[68] Chaudhry, C., Farr, G.W., Todd, M.J., Rye, H.S., Brunger, A.T., Adams, P.D., Horwich, A.L., Sigler, P.B. (2003) *EMBO J.* **22**, 4877-87.

[69] Makino, Y., Amada, K., Taguchi, H., and Yoshida, M. (1997) Chaperonin-mediated folding of green fluorescent protein. *J. Biol. Chem.* **272**, 12468–12474.

[70] Takei, Y., Iizuka, R., Ueno, T., and Funatsu, T. (2012) Single-molecule observation of protein folding in symmetric GroEL-$(GroES)_2$ complexes. *J. Biol. Chem.* **287**, 41118–41125.

[71] Inobe, T., Makio, T., Takasu-Ishikawa, E., Terada, T.P., and Kuwajima, K. (2001) Nucleotide binding to the chaperonin GroEL: non-cooperative binding of ATP analogs and ADP, and cooperative effect of ATP. *Biochim. Biophys. Acta* **1545**, 160–173.

[72] Farr, G.W., Furtak, K., Rowland, M.B., Ranson, N.A., Saibill, H.R., Kirchhausen, T., and Horwich, A.L. (2000) Multivalent binding of nonnative substrate proteins by the chaperonin GroEL. *Cell* **100**, 561–573.

[73] Figueiredo, L., Klunker, D., Ang, D., Naylor, D.J., Kerner, M.J., Georgopoulos, C., Hartl, F.U., Hayer-Hartl, M. (2004) Functional characterization of an archaeal GroEL/GroES chaperonin system: significance of substrate encapsulation. *J. Biol. Chem.* **279**, 1090-9.